ACS OMEGA

Article

Cite This: ACS Omega 2019, 4, 7614−7627

http://pubs.acs.org/journal/acsodf

New Blue Donor−Acceptor Pechmann Dyes: Synthesis, Spectroscopic, Electrochemical, and Computational Studies

Alessio Dessì,*[,†] Adalgisa Sinicropi,[§,†,#] Sanaz Mohammadpourasl,[§,#] Riccardo Basosi,[§,†,#] Maurizio Taddei,[§,†] Fabrizia Fabrizi de Biani,[§] Massimo Calamante,[†,‡] Lorenzo Zani,[†] Alessandro Mordini,[†,‡] Pamela Bracq,[†] Daniele Franchi,[†,‡] and Gianna Reginato*[,†]

[†]Istituto di Chimica dei Composti Organometallici (CNR-ICCOM), Via Madonna del Piano 10, 50019 Sesto Fiorentino, Italy

[‡]Dipartimento di Chimica "U. Schiff", Università degli Studi di Firenze, Via della Lastruccia 13, 50019 Sesto Fiorentino, Italy

[§]Dipartimento di Biotecnologia, Chimica e Farmacia, Università degli Studi di Siena, Via A. Moro 2, 53100 Siena, Italy

[#]CSGI, Consorzio per lo Sviluppo dei Sistemi a Grande Interfase, via della Lastruccia 3, 50019 Sesto Fiorentino, Italy

Supporting Information

ABSTRACT: The design, synthesis, and characterization of a new class of blue-colored thiophene-substituted Pechmann dyes are reported. Due to a distinguishing blue coloration and the capability to absorb light in one of the most photon-dense regions of the solar spectrum, such compounds are of great interest for application as photoactive materials in organic optoelectronics, in particular, in dye-sensitized solar cells. To achieve fine tuning of the optical and electrochemical properties, the electron-poor thiophene-bis-lactone moiety has been decorated with donor (D) and acceptor groups (A), targeting fully conjugated D−A−π−A structures. The designed structures have been investigated by means of DFT and time-dependent DFT calculations, and the most promising dyes have been synthesized. These molecules represent the very first preparation of unsymmetrical Pechmann derivatives. Optical and electrochemical properties of the new dyes have been studied by cyclic voltammetry and UV−vis and fluorescence spectroscopy. In two cases, test cells were built proving that a photocurrent can indeed be generated when using electrolytes especially formulated for narrow-band-gap dyes, although with a very low efficiency.

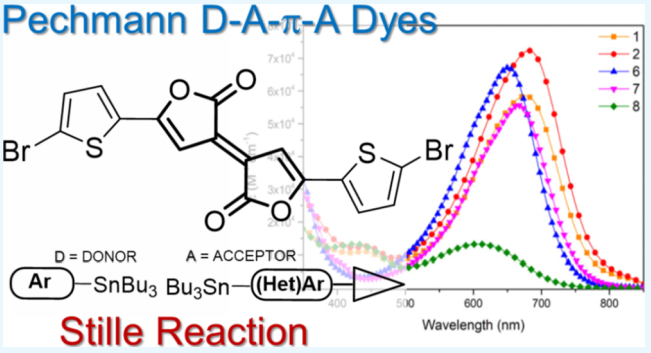

INTRODUCTION

Among new generation photovoltaic technologies, dye-sensitized solar cells (DSSC) are considered a promising option for the efficient conversion of solar energy to electricity.[1] The working principle[2] of a DSSC is inspired by natural photosynthesis as light harvesting is carried out by a dye, which is absorbed on a thin-layer of a mesoporous semiconductor (usually TiO_2). Thanks to photoexcitation, an electron is promoted from the HOMO of the dye to its LUMO and from there is transferred to the conduction band of the semiconductor. Traveling through an external circuit (thus generating an electric current), the electron can be collected at the cathode, where the reduction of a redox couple, such as iodide/triiodide, takes place. The original state of the dye can be finally restored by electron donation from the electrolyte, closing the circuit. Clearly, the photosensitizer represents a key component of a DSSC, being responsible not only for its photovoltaic performances but also for its appearance and for some peculiar properties, such as transparency and color. Accordingly, a large number of metal-free organic dyes have been designed, synthesized, and tested for this kind of application,[3] and in particular, donor−π bridge−acceptor (D−π−A) structures showed desirable characteristics, including tunable optoelectronic and electrochemical properties, simple molecular design, high molar extinction coefficients, low cost, and simple synthetic and purification methods. However, although very good power conversion efficiencies (PCEs) have been reached,[4,5] with record values exceeding 14%,[6] further efforts are required to find colorful, stable, and highly efficient organic dyes, especially when aiming to increase the commercial appeal of DSSC technology for building integration and indoor applications. In particular, blue and green dyes would be of high commercial interest due to their lovely colors, in turn derived from their ability to absorb the incident photons in the red and near-infrared region (NIR) of the spectrum.[7] Nevertheless, although the efficient conversion of low energy photons (λ > 700 nm) is crucial for increasing the overall PCE in a DSSC, only a few blue sensitizers have been reported so far. In particular, some blue devices have been reported using squaraine[8] or diketopyrrolopyrrole

Received: December 19, 2018
Accepted: February 14, 2019
Published: April 26, 2019

DOI: 10.1021/acsomega.8b03560
ACS Omega 2019, 4, 7614−7627

(DPP)-based sensitizers. Above all, the latter were able to give a satisfying efficiency of 7.3% when assembled with the cobalt bipyridine-based electrolytes, a value which was further increased to 8.7% using a co-sensitization strategy with a red dye[9] and even exceeded 10% in the presence of very bulky indoline donors.[10] Very recently, a blue dye featuring an electron-rich polycyclic aromatic hydrocarbon (PAH) scaffold has also been reported achieving a PCE of 12.6%.[11] Clearly, there are still significant possibilities of introducing structural modifications in the sensitizers, in particular, in the search of new building blocks capable of extending the range of available panchromatic dyes. In this context, we have been intrigued by the possibility of introducing the (*E*)-3,3′-bifuranylidene-2,2′-dione heterocyclic systems (Pechmann lactone, Figure 1) in the π scaffold of the dye.

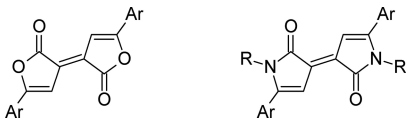

Figure 1. Pechmann and aza-Pechmann molecular structures.

Actually, the Pechmann moiety is characterized by a planar and conjugated structure, which is a known requirement to promote charge transport in organic electronic frameworks. Accordingly, Pechmann bis-lactone and aza-Pechmann bis-lactam units have been exploited to prepare conjugated systems of potential interest for organic electronics,[12,13] for instance, as semiconductors in organic field-effect transistors (OFET).[14] Furthermore, quadrupolar D−A−D systems based on Pechmann-lactone analogues were reported to show highly intense and red-shifted visible−NIR absorption and fluorescence,[15] whereas the aza-Pechmann moiety can be found, together with diketopyrrolopyrrole, in photoactive donor−acceptor polymers suitable for organic photovoltaic devices[16] and also in small molecules that were used to build OFETs with excellent hole mobilities.[17]

In this paper, we report the design of a new family of unsymmetrically substituted Pechmann dyes for application in DSSCs. The dyes studied differ both for the electron-rich substituents on the donor and for the anchoring group (Figure 2). Using an approach which was successfully applied in previous studies,[18] the dyes were investigated by means of

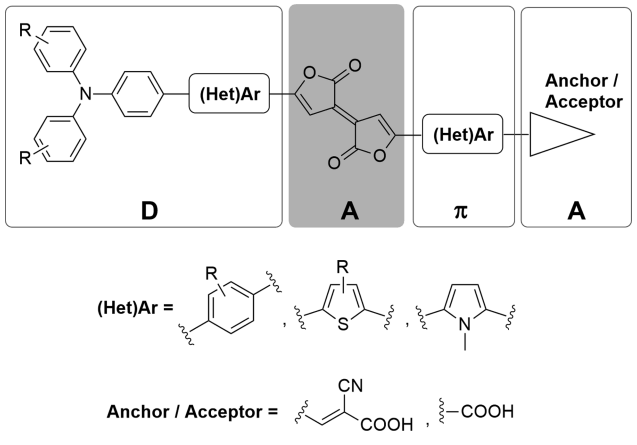

Figure 2. General structure of dyes containing the Pechmann lactone moiety.

density functional theory (DFT) and time-dependent DFT (TD-DFT) calculations, those with the most promising features were synthesized, and their spectroscopic and electrochemical properties were experimentally verified.

RESULTS AND DISCUSSION

Dyes **1**−**13** (Figure 3) were designed with the aim to rationalize the effect of decorating the central Pechmann scaffold with different donor and acceptor groups. We mainly focused on thiophene-derived Pechmann lactones (dyes **1**−**10**) because the thienyl substituent is ubiquitous in the structure of organic semiconductors and photosensitizers. However, to have better insight, some other aromatic and heteroaromatic rings such as xylenyl (**11**), fluorenyl (**12**), and pyrrolyl-(**13**) were considered (Figure 3), and the effect of conjugated spacers with different electron densities was evaluated by placing phenyl (**5** and **6**), ethynylphenyl (**7**), and 3,4-ethylenedioxythiophenyl (EDOT) (**9** and **10**) moieties between the anchoring group and the central core. In addition, hydrophobic alkyl chains were inserted to improve the solubility, reduce aggregation,[19] and simplify the handling of the final compounds. All the structures were endowed with triarylamine donor groups, differing in terms of the presence of electron-rich substituents in the *para* position. In particular, unsubstituted triarylamine compounds (**1** and **8**) were compared with *p*-hexyloxy- (**3**) and *p*-thiohexyl-substituted ones (**2**, **5**, **6**, **7**, **9**, and **10**) because the latter are known to have a beneficial reducing effect on aggregation and enhancing effect on regeneration of the dyes.[19a,b,20,21] Finally, the Pechmann lactone scaffold was substituted with the *aza*-Pechmann one in compounds **4** and **8**.

Computational Studies. To assess the optoelectronic properties of the selected Pechmann-based structures and verify that their energy levels match the semiconductor conduction band and the redox couple potential, it was essential to model the relative energies of their frontier molecular orbitals (FMOs) and their UV−vis absorption maxima. All quantum mechanics (QM) calculations were performed using the Gaussian 09 program package.[22] Geometry optimizations of Pechmann-based dyes (**1**−**13**, Figure 3) were carried out by DFT calculations using the Becke three-parameter-Lee−Yang−Parr (B3LYP) hybrid-DFT exchange-correlation functional[23] in combination with the standard 6-31G* basis set in the gas phase. The values of the HOMO−LUMO energy gaps for all the computed structures are reported along with the wave function plots of corresponding FMOs. Vertical excitation energies (E_{exc}), absorption maxima (λ_{max}), and oscillator strengths (f) were computed at the time-dependent DFT (CAMB3LYP/6-31G*) level on all the optimized structures. To include the effect of the solvent ($CHCl_3$), the polarized continuum model (PCM) was employed.[24] Finally, methyl groups have been used in place of the alkyl chains to reduce the computational cost. The energy and shape of FMOs for **1**−**13** are shown in Figure 4, along with the known D−π−A sensitizer **DF15**,[25] which was used as reference. As we expected, and in comparison to **DF15**, the introduction of the Pechmann unit, which is an auxiliary acceptor group in the π bridge of the molecules, lowered the energy of the LUMO orbitals, consequently reducing the HOMO−LUMO gaps, which were in the range of 1.45−1.78 eV. Similarly to other D−A−π−A dyes,[26] the HOMO/LUMO orbitals of compounds **1**−**13** were mostly localized on the donor and acceptor, respectively, but both also stretched onto

DOI: 10.1021/acsomega.8b03560
ACS Omega 2019, 4, 7614−7627

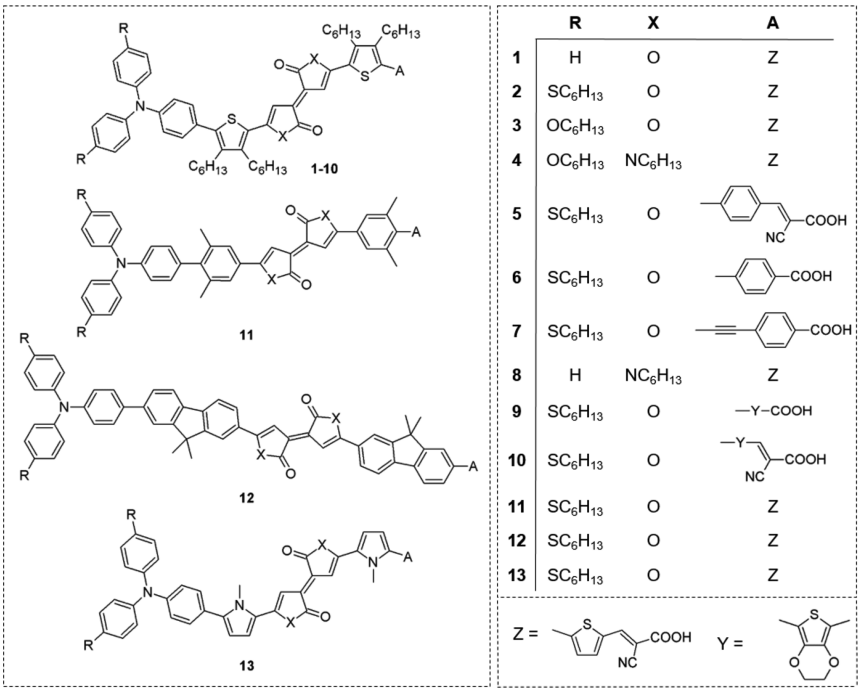

Figure 3. Structures of the designed Pechmann dyes **1**−**13**.

the Pechmann unit, giving rise to an extended superimposition, suggesting strong intramolecular charge transfer upon photoexcitation. Comparing the different structures, it appears that the substitution of the lactone moiety with the less electron-withdrawing lactam (**4** vs **3** and **8** vs **1**) raised the energy of both frontier molecular orbitals, even if the consequent increase of the HOMO−LUMO gap (from 1.49 eV for dye **3** to 1.72 eV for dye **4** and from 1.62 eV for dye **1** to 1.78 eV for dye **8**; see Figure 4) was especially due to the larger positive shift of the LUMO orbital.

As expected, the introduction of a stronger donor group (dyes **2** and **3** vs dye **1**) raised the energy of the HOMO orbital, lowering the HOMO−LUMO gap, whereas the presence of different spacers between the anchoring unit and the central core (dyes **5** and **10** vs dye **2**) affected the energy of the LUMO orbital, with a slight increase of the HOMO−LUMO gap. The same effect was produced by the substitution of the cyanoacrylic acid with a simple carboxylic acid (dyes **6** and **7** vs dye **5**; dye **9** vs dye **10**). In the case of dyes **6** and **7**, the shape of the LUMO was also different, with a smaller contribution of the actual anchoring group, probably as a consequence of the less electron-withdrawing nature of the acceptor. Finally, substitution of the thienyl rings with different aromatic and heteroaromatic moieties (dyes **11**−**13** vs dye **2**) changed the energy levels of both the frontier molecular orbitals, without altering the HOMO−LUMO gap dramatically. Also, in the case of dyes **11** and **12**, we observed a more limited localization of the LUMO on the anchoring group; however, because in this case the latter was the same as those of dyes **1**−**4** and **8**, the reason could not be ascribed to its weaker electron-accepting ability but rather to the smaller planarity of the conjugated system, especially between the π bridge and the acceptor moiety (see Figure S25).

In Table 2, ground- (E^{dye}) and excited ($E^{dye}*$)-state oxidation potentials, electron injection free energies (ΔG^{inject}), and light-harvesting efficiencies (LHE) associated with the oscillator strength (f) of each dye molecule at the maximum absorption wavelength are presented. These photovoltaic properties have been calculated according to the following equations[26]

$$E^{dye} = -E_{HOMO} \quad (1)$$

$$E^{dye}* = E^{dye} - E_{exc} \quad (2)$$

$$\Delta G^{inject} = E^{dye}* - E_{CB} \quad (3)$$

where E_{CB} = −4.0 eV is the conduction band energy of TiO_2.

$$LHE = 1 - 10^{-f} \quad (4)$$

where f is the oscillator strength of the dye.

Assuming that the commonly accepted value is −4.0 eV for the energy of the TiO_2 conduction band,[1] ΔG^{inject} values were negative for all sensitizers, indicating that electron injection from the dye to TiO_2 is predicted to be thermodynamically favored.

The most negative ΔG^{inject} values belong to dyes **11** and **12**, which have also the lowest computed absorption maxima (λ_{max} = 576−585 nm), due to the fact that the most influential electronic transition occurs from the HOMO−1 to LUMO level and to dyes **4**, **6**, and **8**, whose LUMO orbitals have the least negative values. The high and similar values (0.98−0.99) for LHE suggest that all dyes are, in principle, able to maximize the photocurrent response. We can thus conclude that the computational design suggested that almost all of dyes **1**−**13** are suitable sensitizers for DSSC application. In particular, there is an appropriate alignment of the dyes' energy levels: vertical absorption maxima ranging from 600 to 800 nm (except for dyes **11** and **12**) confirm their red to infrared light absorption, high oscillator strength values suggest large molar extinction coefficients, and wave function plots of frontier molecular orbitals involved in the excitation process are in favor of an intramolecular charge-transfer nature of the excitation.

DOI: 10.1021/acsomega.8b03560
ACS Omega 2019, 4, 7614−7627

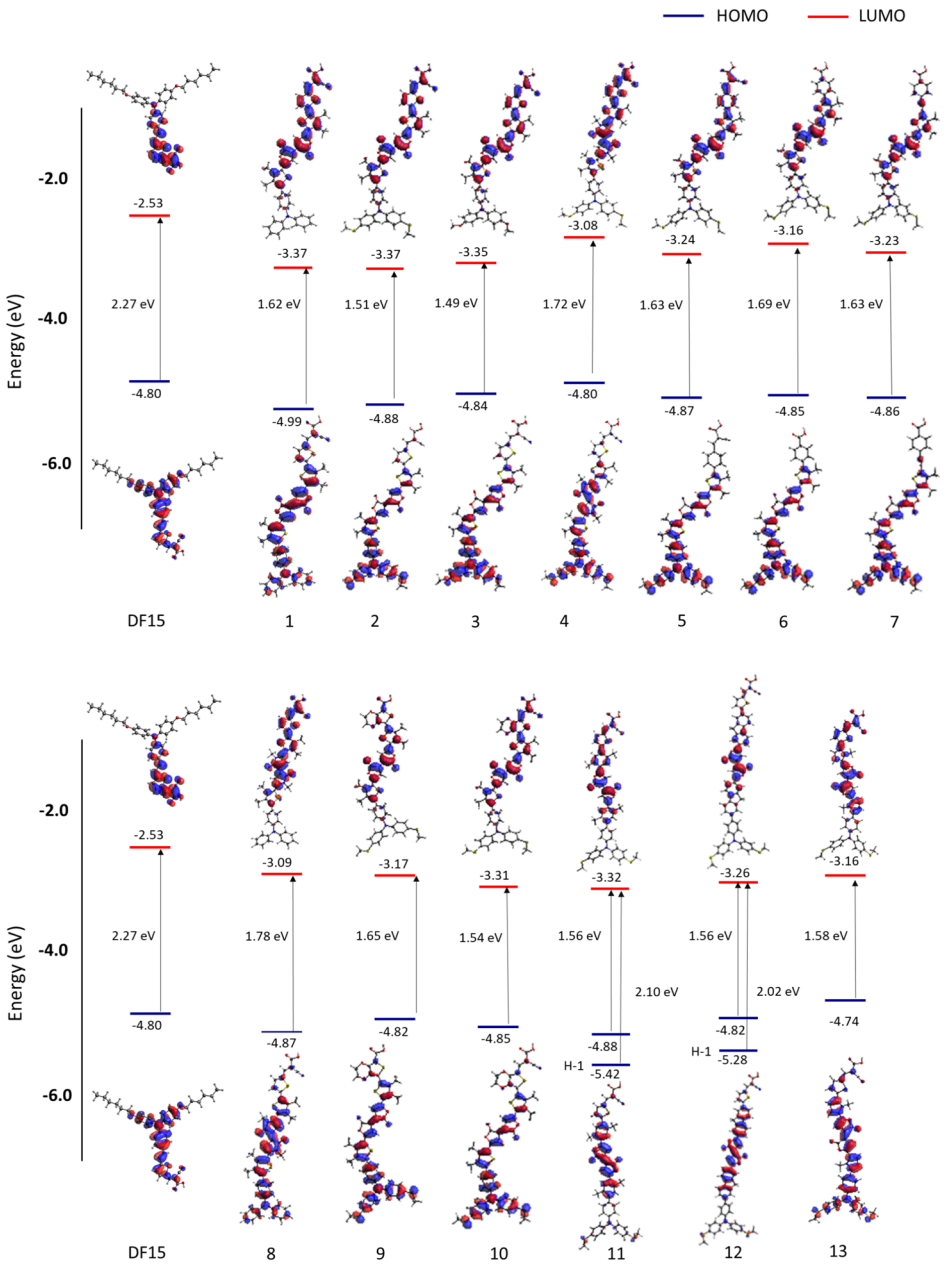

Figure 4. Energy levels and electron density distributions of FMOs of compounds **1**−**13**.

Synthesis of the Pechmann Dyes. Not all the thirteen calculated dyes were synthesized. Taking into account the computational results, we decided to exclude dyes **11** and **12** due to their insufficient NIR light absorption. Among the remaining dyes, we selected compounds **1**, **2**, **6**, **7**, and **8** (see Figure 3). Compound **1** was selected as a reference, and compound **2** was preferred over compound **3** to take advantage of the possible beneficial enhancing effect of thiohexyl chains on dye regeneration.[19b,21] Similarly, between dyes **4** and **8**, where the bis-lactone unit is substituted with the aza-Pechmann core, we selected only compound **8** to be compared with **1**. Finally, we focused on dyes **6** and **7**, having a simple carboxylic anchoring group and less electron-rich phenyl or ethynylphenyl spacers, to be compared with **2**. As mentioned above, in the case of dyes **6** and **7**, the contribution of the actual anchoring groups to their LUMO orbitals was inferior to those shown by the corresponding cyanoacrylic dyes. Nevertheless, we still decided to prepare and test them based on the following considerations: (a) They had more negative calculated ΔG^{inject} values and higher LUMO levels than dyes **1** and **2**, and therefore, we supposed that they could still display a significant charge injection capability owing to a larger driving force. (b) Charge injection into TiO_2 was previously demonstrated also in cases where the LUMO orbital of the dye was spatially separated from the semiconductor surface: an example is the highly performing **ADEKA-1** dye described by Kakiage et al.[6] (for which efficiencies up to 12.5% were reported when used alone).[27] Furthermore, electron transfer to a semiconductor was observed also for dyes (both organic and organometallic) whose main chromophore was separated from the anchoring group by a saturated carbon chain, albeit at a reduced rate compared to the fully conjugated compounds.[28]

DOI: 10.1021/acsomega.8b03560
ACS Omega 2019, 4, 7614−7627

Table 1. TD-DFT (CAM-B3LYP/6-31G*)-Computed Absorption Maxima (λ^{a}_{max})[a]

dyes	λ^{a}_{max} (nm)	E_{exc} (eV)	f	composition (%) H → L
1	675	1.84	2.23	83
2	692	1.79	2.26	72
3	685	1.81	2.27	67
4	639	1.94	1.77	67
5	640	1.94	1.96	65
6	630	1.97	1.79	67
7	652	1.90	2.01	70
8	638	1.94	1.74	79
9	661	1.88	1.91	77
10	684	1.81	2.25	73
11	576	2.15	1.92	72 (H−1 → L)
12	585	2.12	2.59	75 (H−1 → L)
13	700	1.77	2.41	88

[a]Excitation energy (E_{exc}) and oscillator strengths (f) in $CHCl_3$.

Table 2. TD-DFT (CAM-B3LYP/6-31G*)-Computed ΔG^{inject}, LHE, and Ground- (E^{dye}) and Excited (E^{dye*})-State Oxidation Potential Energies

dyes	E^{dye} (eV)	E^{dye*} (eV)	ΔG^{inject} (eV)	LHE
1	4.99	3.16	−0.84	0.99
2	4.88	3.09	−0.91	0.99
3	4.84	3.03	−0.97	0.99
4	4.80	2.86	−1.14	0.98
5	4.87	2.93	−1.07	0.99
6	4.85	2.88	−1.12	0.98
7	4.86	2.95	−1.05	0.99
8	4.87	2.93	−1.07	0.98
9	4.82	2.94	−1.06	0.98
10	4.85	3.04	−0.96	0.99
11	4.88	2.73	−1.27	0.99
12	4.82	2.71	−1.29	0.99
13	4.74	2.96	−1.04	1.00

The synthetic approach to all the dyes started with the preparation of the common intermediate dibromide **17**, which can be obtained, following our optimized procedure,[29] by bromination of thienyl lactone **16**, in turn obtained by reaction of 2,4-dihexylthiophene (**14**) and maleic anhydride (see Scheme 1) and subsequent cyclization of the resulting 4-oxobut-2-enoic acid **15**. Except for a recent polymerization study,[14a] the synthetic elaboration of Pechmann lactones has not been previously reported. In addition, all derivatives described so far are symmetrical, and the desymmetrization of the central Pechmann chromophore to obtain nonsymmetrical D−π−A or similar structures has never been attempted. Very recently, we described the preparation of some symmetrically functionalized Pechmann lactones following a procedure entailing Stille−Migita cross-coupling between dibromide **17** and a suitable stannane.[29] The experimental procedure we used, being performed in very mild conditions and without bases, proved a suitable tool for the synthetic elaboration of the very sensitive bis-lactone scaffold, and thus we decided to use a similar approach also to prepare compounds **1** and **2**. We started with the introduction of the donor groups, which implies the desymmetrization of the central Pechmann scaffold **17**. Reaction with stannanes **18a,b** was then performed, following a slightly modified version of our cross-coupling procedure.[29] Accordingly, the Stille−Migita reactions were carried out using a stoichiometric amount of the stannanes and stopped before the complete conversion of the starting material, to avoid the formation of the symmetric double-coupling product. For this reason, the desired products **19a,b** could be obtained only in 25−27% yield, even though the starting dibromide **17** could always be partially recovered after chromatographic purification, and recycled for further use. The acceptor group was then introduced by a second Stille−Migita reaction using organostannane **20**. In both cases, the desired aldehydes **21a,b** were obtained in good yields. The last step of the synthesis required Knoevenagel condensation to obtain cyanoacrylic acids. Considering that the Pechmann core proved to be quite sensitive to the presence of excess acetic acid, we needed to modify the standard reaction conditions, which commonly require using a mixture of toluene and acetic acid as the solvent and a large excess of cyanoacetic acid and ammonium acetate.[30] Instead, we decided to use a stoichiometric amount of piperidine[25] as the base and a mixture of toluene and acetonitrile as the solvent. In this way, provided that the reaction is stopped before the complete conversion of the starting materials to minimize degradation, we have been able to recover the desired dyes **1** and **2** in 37 and 62% isolated yield, respectively (Scheme 2).[1]

Advanced intermediate **19b** was also used to prepare the two dyes **6** and **7** (Scheme 3). Following the usual procedure, reaction with organostannane **22**[31] gave compound **6** in good yield after purification (Scheme 3).On the other hand, compound **7** was prepared by coupling **19b** with the unprotected 4-ethynylbenzoic acid **23**, following standard Sonogashira conditions, that is, $Pd(PPh_3)_4$ as the catalyst, CuI as the co-catalyst, and Et_3N as the base.[32]

Finally, to synthesize compound **8**, lactone **16** was reacted overnight with a 4-fold excess of n-$C_6H_{13}NH_2$ and 20% DMAP in DCM, followed by acidification with $TsOH{\cdot}H_2O$ (Scheme 4)[13a] to obtain lactam **25**. Unfortunately, attempts to prepare dibromide **24** by standard bromination of **25** failed, and only decomposition products were recovered even after a very short reaction time. Therefore, we decided to convert directly dibromo bis-lactone **17** into bis-lactam **24**. Using the same amidation conditions, pure intermediate **24** was indeed recovered after chromatography, although in moderate yield. To end the synthesis, the usual approach was followed,

Scheme 1. Synthetic Pathway for the Preparation of the Pechmann Scaffold

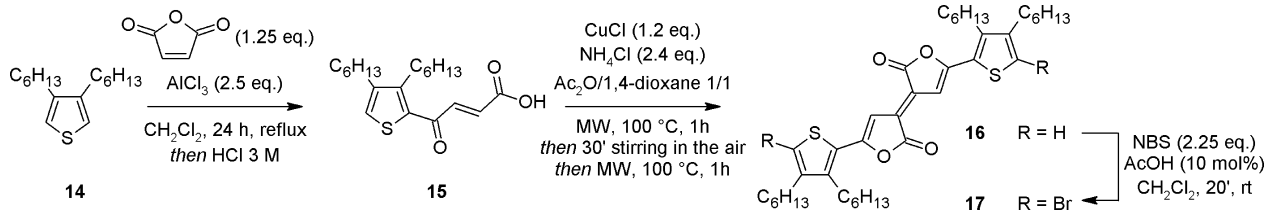

DOI: 10.1021/acsomega.8b03560
ACS Omega 2019, 4, 7614−7627

Scheme 2. Preparation of Nonsymmetrical Pechmann Derivatives 1 and 2

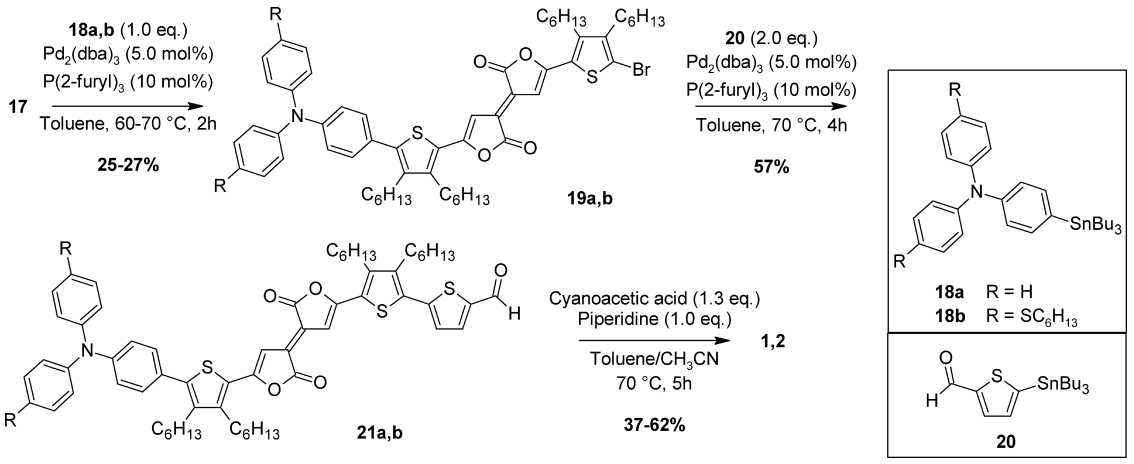

Scheme 3. Preparation of Nonsymmetrical Pechmann Derivatives 6 and 7

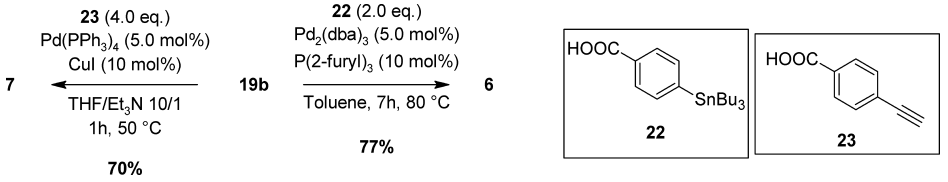

Scheme 4. Preparation of Aza-Pechmann Derivative 8

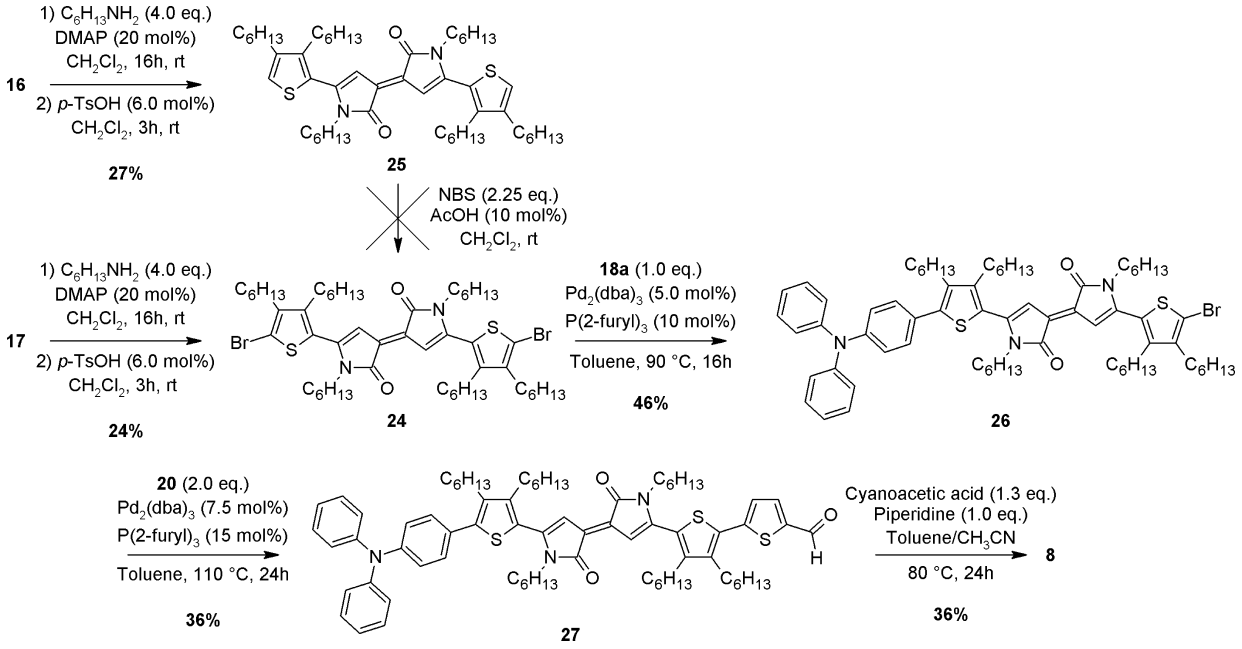

performing two subsequent cross-coupling reactions, using stannane **18a** first and then stannane **20**. Although in both cases, lactam derivatives showed a lower reactivity compared to their lactone analogues and higher reaction temperature and longer times were required, the desired dye **8** was indeed obtained in a pure form and with a reasonable overall yield. Surprisingly, dye **8** was quite unstable, rapidly turning from green (see below) to pale yellow upon dissolution in the most common solvents. We tentatively attribute such behavior to the ring opening of the lactam moiety (possibly followed by ring closure to a different isomer), which has been reported to yield species characterized by weaker and blue-shifted absorption spectra compared to the Pechmann chromophore.[12,13]

Spectroscopic and Electrochemical Data. The optical properties of all the new dyes were studied. First of all, the UV−vis spectra of dye **1** and all its synthetic intermediates containing the Pechmann moiety (namely, **16**, **17**, **19a**, and **21a**) were recorded in $CHCl_3$ solution (Figure 5a). The comparison clearly shows the red shift and widening of the absorption bands, due to the elongation of the conjugated skeleton and the formation of the alternating D−A structure,

DOI: 10.1021/acsomega.8b03560
ACS Omega 2019, 4, 7614−7627

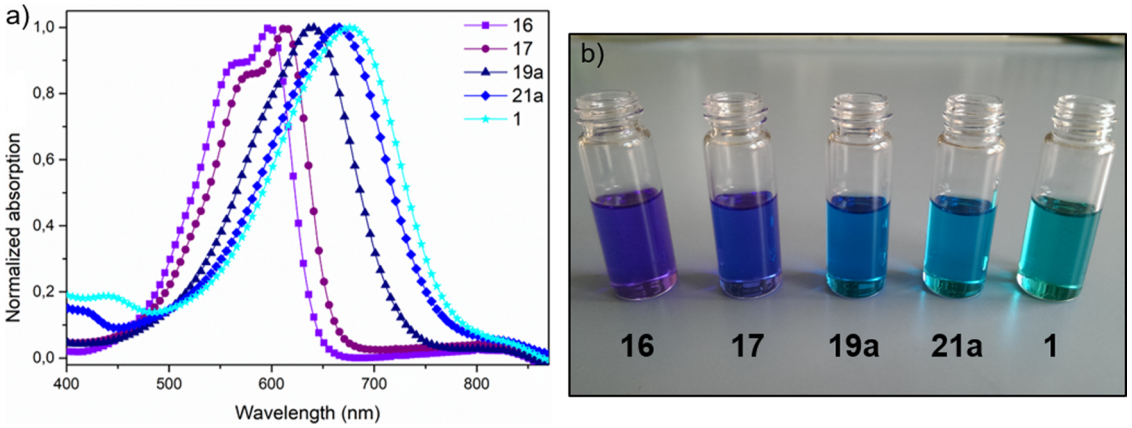

Figure 5. (a) UV−vis absorption spectra of intermediates **16**, **17**, **19a**, and **21a** and of dye **1** in $CHCl_3$: **16**, violet squares; **17**, purple circles; **19a**, navy blue triangles; **21a**, blue diamonds; and **1**, cyan stars. (b) Photograph of $CHCl_3$ solutions of compounds **16**, **17**, **19a**, **21a**, and **1** (approximate concentration of 1−2 × 10^{-5} M).

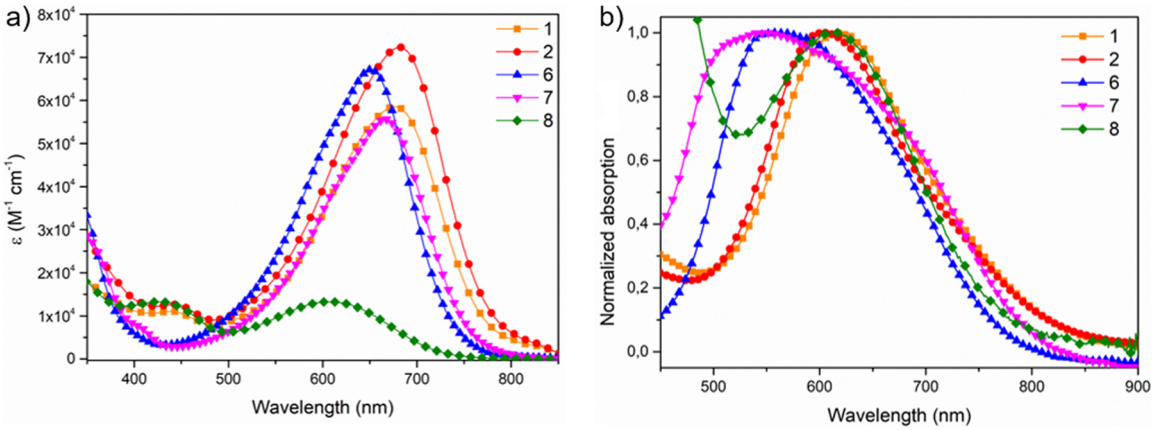

Figure 6. (a) UV−vis absorption spectra of compounds **1**, **2**, **6**, **7**, and **8** in $CHCl_3$ solution. (b) Normalized UV−vis absorption spectra of compounds **1**, **2**, **6**, **7**, and **8** adsorbed on a TiO_2 thin film: **1**, orange squares; **2**, red circles; **6**, blue upside triangles; **7**, purple downside triangles; and **8**, green rhombi.

Table 3. Spectroscopic and Electrochemical Data for Dyes 1, 2, 6, 7, and 8

compound	$\lambda_{abs.}$ (nm)[a]	ε (× 10^4) [M^{-1} cm^{-1}]	$\lambda_{abs.}$ (nm) on TiO_2	λ_{emi} (nm)[a]	E_{0-0} (eV)[b]	$E_{S+/S}$ (V)[c]	E_{S+/S^*} (V)[d]	Γ (× 10^{-7}) [mol cm^{-2}]
1	676	5.9	617	799	1.68	1.10	−0.58	1.88
2	681	7.2	604	788	1.69	1.05	−0.64	2.47
6	651	6.8	558	754	1.78	1.03	−0.75	0.50
7	666	5.6	550	766	1.75	1.02	−0.73	1.02
8[e]	608 (433)	1.6 (2.0)	612 (413)	742	1.80			0.82

[a]In $CHCl_3$ solution. [b]Estimated from the intersection of normalized absorption and emission spectra. [c]Measured in 0.1 M CH_2Cl_2/$TBAPF_6$ on a glassy carbon electrode. Values are reported against NHE. [d]Obtained by means of the following expression: $E_{S+/S^*} = E_{S+/S} - E_{0-0}$. [e]$E_{S+/S}$ and E_{S+/S^*} were not measured due to decomposition of compound **8**.

with the color of the compounds progressively shifting from violet to cyan (Figure 5b). This trend was finely predicted by the TD-DFT study (see Supporting Information, Table S2). UV−vis spectra of dyes **1**, **2**, **6**, **7**, and **8** were then recorded, both in $CHCl_3$ solution and after adsorption on TiO_2 (Figure 6a,b and Table 3). Again, the values we found are in very good agreement with those obtained from the DFT/TD-DFT study (Table 1). As expected, **1**, **2**, **6**, and **7** showed an intense cyan color in solution due to their broad absorption of red/NIR light. In particular, dyes **1** and **2** showed the most red-shifted absorption with a maximum value of λ = 681 nm registered for **2**, due to the strong electron-donating character of the thioalkyl substituent. On the other hand, the presence of less electron-withdrawing anchoring groups such as for dyes **6** and **7** resulted in a blue shift of the absorption maxima, which is more pronounced in the case of **6** probably because of a loss of planarity, which might hamper conjugation between the thienyl group of the central scaffold and the benzoic acid substituent. Finally, bis-lactam-based compound **8** presented a blue-shifted and much less intense low-energy absorption band compared to its bis-lactone analogue **1** (1.6 × 10^4 vs 5.9 × 10^4 M^{-1} cm^{-1}), which was accompanied by a higher energy absorption band of similar intensity (2.0 × 10^4 M^{-1} cm^{-1}) at 433 nm. As a consequence, the corresponding $CHCl_3$ solution displayed an intense green rather than cyan color (Figure 6a).

DOI: 10.1021/acsomega.8b03560
ACS Omega 2019, 4, 7614−7627

All dyes exhibited fluorescence in $CHCl_3$ solution (Figures S26−S30); therefore, optical band gaps (E_{0-0}) could be obtained from the intersection of the normalized absorption and emission spectra and were found in the 1.68−1.80 eV range (Table 3), with **1** and **2** having the smallest E_{0-0} values. A very wide absorption band (500−850 nm) was observed when the dyes were adsorbed on the TiO_2 layer. This was accompanied by a moderate blue shift of the maximum absorption peak, probably due to partial aggregation.[33] Interestingly, the only exception was observed for dye **8**, for which a slight red shift was observed (612 vs 608 nm in $CHCl_3$ solution), possibly due to the presence of two additional linear hexyl chains (bonded to the lactam nitrogen atoms) on its molecular structure, which might have a limiting effect on the incidence of aggregation phenomena.[19a,b] As already outlined, in the case of dye **8**, we observed a rapid change in color from green to pale yellow after dissolution in most of the common solvents or adsorption on TiO_2 which hampered any further analysis. The ground-state oxidation potentials ($E_{S+/S}$) of the dyes were then measured by means of cyclic voltammetry (CV), which was carried out in dichloromethane solutions in the presence of 0.1 M Bu_4NPF_6 as the electrolyte (Figures S31−S34 and Table 3).

$E_{S+/S}$ values ranging from 1.02 to 1.10 V versus the normal hydrogen electrode (NHE) were found, and consequently, driving forces for the regeneration from the I^-/I_3^- redox couple (ΔG_{reg}) were over 670 mV.

Because overpotentials of approximately 500 mV are required for efficient dye regeneration from the iodide/triiodide electrolyte,[34] the electron transfer from the redox shuttle to the oxidized dyes is expected to work well. Indeed, the excited-state oxidation potential ($E_{S+/S*}$) is a crucial parameter to assess the electron injection efficiency from the excited state of the dye to the conduction band (CB) of titania and was calculated using the following equation

$$E_{S+/S*} = E_{S+/S} - E_{0-0}$$

All the calculated $E_{S+/S*}$ values are in the range −0.58 to −0.75 V versus NHE (Table 3). In Figure 7, the comparison of ground-state and excited-state oxidation potentials of dyes **1** and **2** and **6** and **7** with the TiO_2 CB (−0.50 V vs NHE) and the iodide/triiodide redox couple (0.35 V vs NHE)[35] potentials is reported, together with that of the **DF15** reference dye.[25] Clearly, the driving force for electron injection (ΔG^{inject}) ranges from ∼80 to 250 mV, values that are lower than 300 mV, which is the optimal driving force to have fast kinetics of electron injection in the TiO_2 layer,[7,34] but are comparable or superior to the minimum overpotential, which is estimated to be ∼100 to 150 mV (Figure 7).[34,36]

This situation is unfortunately common in narrow-band-gap dyes, especially those containing strong electron-deficient π bridges (see for instance thieno[3,4-*b*]pyrazine-based dyes),[18d,37] resulting in low efficiency of the corresponding devices. Very often, in these cases, the ΔG^{inject} can be increased by using special precautions in fabricating solar cells.

Photovoltaic Measurements. To assess the capability of the new compounds to yield working DSSCs, we decided to carry out a preliminary study and built some solar devices using dyes **6** and **7**. We selected these two dyes because, relying on the values of excited state potentials ($E_{S+/S*}$), they were the only ones able to guarantee the minimum required overpotential with respect to the TiO_2 conduction layer, with

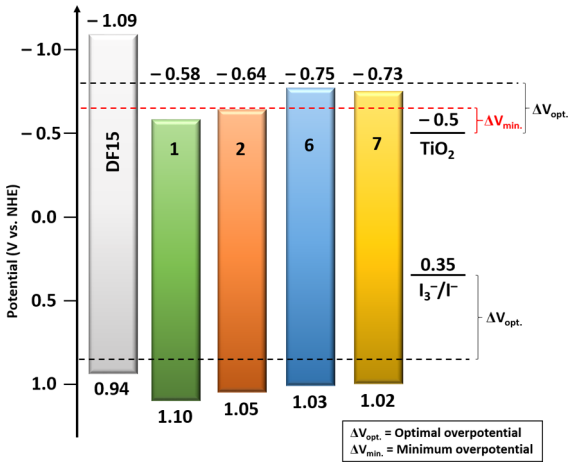

Figure 7. Energy level diagram of ground-state and excited-state oxidation potentials of dyes **DF15**, **1**, **2**, **6**, and **7** compared with TiO_2 CB (−0.50 V) and iodide/triiodide redox couple (0.35 V) potentials. Black dotted lines mark the optimal $E_{S+/S}$ (0.85 V) and $E_{S+/S*}$ (−0.80 V) values for a sensitizer with fast electron transfer kinetics. The red dotted line defines the limit potential (−0.65 V) to guarantee electron injection.

dye **8** being too unstable to be used in the experimental conditions required.

Initially, we built test cells using standard conditions: photoanodes of different thicknesses were sensitized with compound **6**, and a standard high-performance electrolyte[38] was used. No photocurrent was recorded in such conditions. However, the electrolyte we used contains special additives (i.e., *tert*-butyl pyridine and guanidinium isothiocyanate GuSCN), which are usually present with the aim of increasing V_{oc} by enhancing the TiO_2 CB potential. This feature is not compatible with dyes having a low injection overpotential; thus, we decided to try to investigate different electrolyte compositions. In particular, six different electrolytes were tested, sensitizing the electrodes with dye **6**, and the three best-performing compositions were also tested using dye **7**. The power conversion efficiency, η, was calculated using the following equation

$$\eta = J_{sc} V_{oc} FF / I_0 \quad (5)$$

where J_{sc} is the short-circuit photocurrent density, V_{oc} is the open-circuit photovoltage, FF is the fill factor, and I_0 is the energy of incident sunlight (100 mW cm^{-2}). The results obtained are summarized in Table 4. It is evident that for all the cells prepared, a very low efficiency was recorded; however, in the case of dye **6**, even with a simple electrolyte containing only the redox couple (A), a low photocurrent was observed. LiI and guanidinium thiocyanate were then added, which are often used to increase both V_{oc} and the short-circuit photocurrent (J_{sc}).[39,40] Indeed, a moderate concentration of guanidinium thiocyanate (B) increased V_{oc} values without affecting the photocurrent, whereas a higher concentration of guanidinium thiocyanate (C) was detrimental to both. Addition of the bulky cation 1-butyl-3-methylimidazolium (BMI^+) and the innocent anion ClO_4^- (D), as expected, slowed down the recombination processes increasing the photovoltage;[41] however, it did not give a better efficiency. Increasing the concentration of Li^+ to 1.025 M (E) and 1.625 M (F) gave, as we expected, higher photocurrents, with the best results occurring with electrolyte E, corresponding also

DOI: 10.1021/acsomega.8b03560
ACS Omega 2019, 4, 7614−7627

Table 4. Photovoltaic Characteristics of the DSSC Sensitized with Dyes 6 and 7 under AM 1.5 Simulated Solar Illumination

dye	E[a]	J_{sc} (mA cm^{-2})	V_{oc} (mV)	FF	η (%)[b]
6	A	0.86	386.0	52.0	0.17
7		0.63	412.6	53.4	0.14
6	B	0.84	400.6	54.0	0.18
7		0.54	408.1	43.4	0.10
6	C	0.65	362.9	40.7	0.10
6	D	0.68	430.6	57.2	0.17
6	E	1.19	420.8	48.9	0.24
7		0.53	387.4	44.7	0.10
6	F	0.95	414.3	44.2	0.17

[a]Electrolyte: A: I_2 (0.04 M), LiI (0.625 M); B: I_2 (0.04 M), LiI (0.625 M), guanidinium thiocyanate (0.1 M); C: I_2 (0.04 M), LiI (0.625 M), guanidinium thiocyanate (0.3 M); D: I_2 (0.04 M), *N*-methyl-*N*-butylimidazolium iodide (0.625 M), $LiClO_4$ (0.625 M), guanidinium thiocyanate (0.1 M); E: I_2 (0.04 M), LiI (0.625 M), guanidinium thiocyanate (0.1 M), $LiClO_4$ (0.4 M); F: I_2 (0.04 M), LiI (0.625 M), guanidinium thiocyanate (0.1 M), $LiClO_4$ (1.0 M). In all cases, the solvent was acetonitrile/valeronitrile (85/15, v/v). [b]Data refer to the best results obtained for at least three devices for each configuration.

with the best efficiency recorded. When electrodes were sensitized with dye **7**, the effect of the additives was detrimental in all cases, and cells built using the simple electrolyte A resulted in the best performing ones. This different behavior of dye **7** might be due to its lower excited state potential (see Table 3), which makes any attempt to enhance the electron injection process ineffective. Representative *J*/*V* curves for the best devices built with dyes **6** and **7** are reported in Figure S35.

In any case, the low efficiencies recorded were mostly due to low photocurrents. Recalling the results of our computational analysis, it is possible that the scarce delocalization of the LUMO orbitals of dyes **6** and **7** on their actual anchoring groups, coupled with the abovementioned small driving forces, limited their charge injection efficiency, reducing its rate and making it competitive with recombination reactions as well as unproductive intermolecular energy transfer processes.

CONCLUSIONS

Thirteen new thiophene-substituted Pechmann dyes have been designed, intended to evaluate the effect of decorating the central scaffold with different donor (D) and acceptor (A) groups on their physico- and electrochemical properties. Such an approach was aimed at preparing new D−A−π−A structures suitable for application as sensitizers for DSSCs because increased knowledge in choosing an appropriate combination of D/A moieties and exploitation of new building blocks are essential for the development of high-performance devices.

The designed structures were investigated by means of DFT and TD-DFT calculations to evaluate the red to NIR absorption maxima, the proper alignment of their FMO energies compared to the CB of TiO_2 and the I^-/I_3^- redox potential, and the intramolecular charge-transfer nature of the excitation. Calculations suggested that almost all the designed dyes were suitable for application in DSSCs. Five of these new dyes were prepared using an approach that was based on bromination of the central Pechmann core and desymmetrization by running Stille−Migita cross-coupling in strictly stoichiometric conditions and stopping the reaction before complete consumption of the starting material. Further elaboration of the resulting intermediates led to the preparation of D−A−π−A compounds constituting, to the best of our knowledge, the first example of synthesis of unsymmetrical Pechmann (or aza-Pechmann) derivatives. In agreement with DFT computational studies, the new dyes showed intense absorption of light in the NIR region of the spectrum, accompanied by a significant degree of intramolecular charge transfer. Unfortunately, the driving force for electron injection (ΔG^{inject}) of such dyes was found to be too low to have fast kinetics of electron injection. This is in agreement with the very low efficiencies given by test cells built using two representative dyes (**6** and **7**), whose charge injection capabilities were also probably hampered by insufficient LUMO delocalization, caused by the weak electron-withdrawing nature of their anchoring groups. Nevertheless, a photocurrent increase could still be observed in the presence of electrolytes especially formulated for narrow-band-gap dyes with low $E_{S+/S*}$. The results of these preliminary investigations provide a basic understanding of the properties of D−A−π−A dyes based on the Pechmann chromophore and should be useful to stimulate further research directed toward structural refinement of the sensitizers and optimization of device characteristics.

EXPERIMENTAL SECTION

Unless otherwise stated, all reagents were purchased from commercial suppliers and used without purification. Dibromide **17** and stannanes **18a**, **18b**, **20**,[29] and **22**[31a] were prepared as reported. All air-sensitive reactions were performed using Schlenk techniques. Solvents used in cross-coupling reactions were previously degassed by means of the "freeze−pump−thaw" method. Tetrahydrofuran (THF) was freshly distilled immediately before use from sodium/benzophenone. CH_2Cl_2 and triethylamine were distilled over CaH_2, and toluene and acetonitrile were dried on a resin exchange solvent purification system. Petroleum ether, unless specified, is the 40−70 °C boiling fraction. Reactions were monitored by TLC on SiO_2 plates, and detection was made using a $KMnO_4$ basic solution or a UV lamp. The organic phase derived from aqueous workup was dried over Na_2SO_4. Flash column chromatography was performed using glass columns (10−50 mm wide) and SiO_2 (230−400 mesh).^{1}H-NMR spectra recorded at 300 or 400 MHz and ^{13}C-NMR spectra were recorded at 75.5 or 100.6 MHz, respectively. Chemical shifts were referenced to the residual solvent peak ($CDCl_3$, δ 7.26 ppm for ^{1}H-NMR and δ 77.16 ppm for ^{13}C-NMR; THF-d_8, δ 1.72 and 3.58 ppm for ^{1}H-NMR and δ 67.21 and 25.31 ppm for ^{13}C-NMR; C_6D_6, δ 7.16 ppm for ^{1}H-NMR and δ 128.06 ppm for ^{13}C-NMR). Coupling constants (*J*) were reported in Hz. ESI-MS analyses were recorded with an LCQ-Fleet ion-trap mass spectrometer. HR-MS analyses were performed using a LTQ Orbitrap FT-MS spectrometer. FT-IR spectra were recorded with a Perkin-Elmer Spectrum BX instrument in the range 4000−400 cm^{-1} with 2 cm^{-1} resolution. UV−vis spectra were recorded with a Varian Cary 400 spectrometer and a Shimadzu 2600 series spectrometer, and fluorescence spectra were recorded with a Varian Eclipse instrument, irradiating the sample at the wavelength corresponding to the maximum absorption in the UV spectrum. In all electrochemical experiments, N_2-saturated solutions of the compound under study were used with $[Bu_4N][PF_6]$ (0.1 M) as the supporting electrolyte (Fluka, electrochemical grade) and

DOI: 10.1021/acsomega.8b03560
ACS Omega 2019, 4, 7614−7627

freshly distilled dichloromethane. Cyclic voltammetry was performed in a three-electrode cell using a glassy carbon working electrode, a platinum counter electrode, and a AgCl/Ag (NaCl 3 M) reference electrode. A BAS 100 W electrochemical analyzer was used as the polarizing unit. All the potential values are referred to the NHE ([E vs NHE] = [E vs Ag/AgCl (NaCl 3 M) +0.21] V). Typical analyte concentration was 10^{-3} M. Ferrocene was used as the external standard (+0.44 V vs Ag/AgCl).

General Procedure for Preparation of Compounds 19a,b. Dibromide **17** (1.0 equiv) was dissolved in toluene, and then a solution of Pd_2dba_3 (5 mol %) and P(2-furyl)$_3$ (10 mol %) in toluene and the appropriate stannane (**18**, 1.0 equiv) were added. The resulting mixture was heated to 70 °C, stirred for 2 h, then allowed to cool to rt, and diluted with H_2O (50 mL) and ethyl acetate (100 mL). The organic layers were washed with brine and dried. After filtration and evaporation of the solvent, the crude product was purified by flash column chromatography.

*(3E)-5-(5-(4-(Diphenylamino)phenyl)-3,4-dihexylthiophen-2-yl)-5′-(5-bromo-3,4-dihexylthiophen-2-yl)-3,3′-bifuranyl idene-2,2-dione (**19a**).* Dibromide **17** (185 mg, 0.23 mmol) in toluene (15 mL) was dissolved and reacted with $Pd_2(dba)_3$ (12 mg, 0.011 mmol), P(2-furyl)$_3$ (5.2 mg, 0.022 mmol), and 4-tributylstannyl-*N*,*N*-diphenylaniline (**18a**, 120 mg, 0.23 mmol) at 70 °C. Flash column chromatography (petroleum ether/toluene gradient of 6:1 to 2:1) gave pure product **19a** (56 mg, 0.056 mmol, 25% yield) as a dark-blue amorphous solid. ^{1}H-NMR (400 MHz, $CDCl_3$): δ = 7.27−7.33 (m, 7H), 7.23 (s, 1H), 7.15 (d, J = 7.5 Hz, 4H), 7.06−7.10 (m, 4H), 2.81−2.85 (m, 4H), 2.51−2.62 (m, 4H), 1.47−1.66 (m, 12H), 1.24−1.43 (m, 20H), 0.79−0.91 (m, 12H) ppm; ^{13}C-NMR (75 MHz, $CDCl_3$): δ = 167.2, 166.9, 155.0, 152.8, 148.7, 148.3, 147.4, 145.8, 145.5, 144.5, 141.0, 129.9, 129.6, 127.3, 126.3, 125.3, 125.2, 124.0, 123.8, 123.5, 122.5, 116.6, 104.1, 104.0, 31.7, 31.6, 31.5, 31.0, 30.2, 30.0, 29.9, 29.7, 29.6, 29.5, 29.4, 28.5, 27.4, 22.7, 14.2 ppm; IR (KBr): $\tilde{\nu}$ = 3029, 2924, 2853, 1762, 1559, 1199 cm^{-1}; ESI-MS: m/z = 987.28 [M+1]$^+$

*(3E)-5-(5-(4-(Di(4-(hexylthio)phenyl)amino)phenyl)-3,4-dihexylthiophen-2-yl)-5′-(5-bromo-3,4-dihexyl thiophen-2-yl)-3,3′-bifuranylidene-2,2′-dione (**19b**).* Dibromide **17** (180 mg, 0.22 mmol) was dissolved in toluene (12 mL) and reacted with $Pd_2(dba)_3$ (11 mg, 0.011 mmol), P(2-furyl)$_3$ (5.1 mg, 0.021 mmol), and 4-tributylstannyl-*N*,*N*-(4-hexylthiophenyl) aniline (**18b**, 168 mg, 0.22 mmol) at 60 °C. Flash column chromatography (petroleum ether/toluene gradient of 6:12 to 2:1) gave pure product **19b** (72 mg, 0.059 mmol, 27% yield) as a blue gummy solid. ^{1}H-NMR (300 MHz, C_6D_6): δ = 7.47 (s, 1H), 7.31−7.38 (m, 3H), 7.25 (d, J = 8.7 Hz, 4H), 7.06 (d, J = 8.6 Hz, 2H), 6.98 (d, J = 8.6 Hz, 4H), 2.81−2.92 (m, 2H), 2.58−2.76 (m, 8H), 2.40−2.49 (m, 2H), 1.70−1.82 (m, 2H), 1.05−1.68 (m, 46H), 0.95−1.02 (m, 6H), 0.79−0.94 (m, 12H) ppm; ^{13}C-NMR (75 MHz, C_6D_6): δ = 166.8, 166.5, 155.0, 153.0, 148.4, 148.3, 145.6, 145.4, 145.3, 144.5, 141.0, 132.6, 131.4, 131.0, 130.4, 125.8, 125.5, 125.0, 124.8, 124.0, 122.8, 116.7, 104.43, 104.39, 34.4, 31.94, 31.87, 31.76, 31.66, 31.3, 30.4, 30.2, 30.1, 30.0, 29.9, 29.8, 29.7, 29.6, 28.8, 28.6, 27.7, 23.13, 23.07, 23.0, 22.9, 14.39, 14.36, 14.31, 14.25 ppm; IR (KBr): $\tilde{\nu}$ = 3014, 2927, 2855, 1762, 1560, 1199 cm^{-1}. ESI-MS: m/z = 1220.32 [M+1]$^+$

General Procedure for Preparation of Compounds 21a,b. Bromide (**19a**,**b**, 1.0 equiv) was dissolved in toluene and reacted with a solution of Pd_2dba_3 (5 mol %), P(2-furyl)$_3$ (10 mol %), and 2-tributylstannyl-5-formylthiophene (**20**, 2.0 equiv) in toluene. The resulting mixture was heated to 70 °C and stirred for 4 h, and then it was cooled to rt and diluted with H_2O (50 mL) and ethyl acetate (100 mL). The organic layer was washed with brine and dried. After filtration and evaporation of the solvent, the crude product was purified by flash column chromatography.

*(3E)-5-(5-(4-(Diphenylamino)phenyl)-3,4-dihexylthiophen-2-yl)-5′-(5-(5-formylthiophen-2-yl)-3,4-dihexylthiophen-2-yl)-3,3′- bifuranylidene-2,2′-dione (**21a**).* Bromide **19a** (73 mg, 0.074 mmol) was dissolved in toluene (9 mL) and reacted with $Pd_2(dba)_3$ (3.8 mg, 0.004 mmol, 5 mol %), P(2-furyl)$_3$ (1.7 mg, 0.007 mmol, 10 mol %), and 2-tributylstannyl-5-formylthiophene (**20**, 59 mg, 0.148 mmol). Flash column chromatography (petroleum ether/toluene gradient, 2:1 to 1:3) gave pure aldehyde **21a** (43 mg, 0.042 mmol, 57% yield) as an amorphous black solid. ^{1}H-NMR (400 MHz, $CDCl_3$): δ = 9.91 (s, 1H), 7.73 (d, J = 4.0 Hz, 1H), 7.34 (s, 1H), 7.27−7.33 (m, 8H), 7.15 (d, J = 7.7 Hz, 4H), 7.06−7.10 (m, 4H), 2.66−2.88 (m, 6H), 2.57−2.64 (m, 2H), 1.48−1.66 (m, 16H), 1.25−1.42 (m, 16H), 0.85−0.94 (m, 12H) ppm; ^{13}C-NMR (100 MHz, $CDCl_3$): δ = 182.7, 167.1, 166.9, 155.3, 152.7, 149.0, 148.4, 147.6, 147.4, 145.9, 145.2,143.6, 143.5, 141.1, 136.7, 134.6, 129.9, 129.6, 127.4, 127.2, 126.5, 125.6, 125.3, 124.0, 123.8, 123.2, 122.4,105.3, 104.2, 31.7, 31.64, 31.61, 31.5, 31.0, 30.5, 30.2, 30.0, 29.9, 29.8, 29.7, 29.5, 29.4, 29.1, 28.2, 27.5, 22.79, 22.77, 22.74, 22.72, 14.2 ppm; IR (KBr): $\tilde{\nu}$ = 3062, 2924, 2854, 1757, 1661, 1551, 1201 cm^{-1}; ESI-MS: m/z = 1063.70 [M+C_2H_6O]$^+$.

*(3E)-5-(5-(4-(bis(4-(Hexylthio)phenyl)amino)phenyl)-3,4-dihexylthiophen-2-yl)-5′-(5-(5-formylthiophen-2-yl)-3,4-dihexylthiophen-2-yl)-3,3′-bifuranylidene-2,2′-dione (**21b**).* Bromide **19b** (90 mg, 0.074 mmol) was dissolved in toluene (10 mL) and reacted with $Pd_2(dba)_3$ (3.8 mg, 0.004 mmol, 5 mol %), P(2-furyl)$_3$ (1.7 mg, 0.007 mmol, 10 mol %), and 2-tributylstannyl-5-formylthiophene (**20**, 59 mg, 0.148 mmol). Flash column chromatography (petroleum ether/toluene, gradient 2:1 to 1:3) gave pure aldehyde **21b** (52 mg, 0.042 mmol, 57% yield) as a blue gummy solid. ^{1}H-NMR (300 MHz, C_6D_6): δ = 9.46 (s, 1H), 7.49 (s, 1H), 7.48 (s, 1H), 7.35 (d, J = 8.3 Hz, 2H), 7.25 (d, J = 8.3 Hz, 4H), 7.07 (d, J = 8.6 Hz, 2H), 6.98 (d, J = 8.4 Hz, 4H), 6.93 (d, J = 3.8 Hz, 1H), 6.84 (d, J = 3.8 Hz, 1H), 2.82−2.94 (m, 2H), 2.56−2.79 (m, 10H), 1.68−1.82 (m, 2H), 1.05−1.68 (m, 46H), 0.95−1.02 (m, 6H), 0.79−0.94 (m, 12H) ppm; ^{13}C-NMR (75 MHz, C_6D_6): δ = 181.8, 166.8, 166.6, 155.2, 153.1, 148.7, 148.3, 147.7, 145.6, 145.4, 144.3, 144.1, 143.4, 141.1, 136.1, 135.2, 132.7, 131.0, 130.4, 127.4, 126.8, 125.9, 125.7, 124.9, 123.8, 122.8, 105.6, 104.5, 34.4, 32.0, 31.9, 31.74, 31.66, 31.3, 30.5, 30.4, 30.2, 30.1, 29.8, 29.6, 29.3, 28.8, 28.3, 27.7, 23.1, 23.0, 22.9, 14.4, 14.3, 14.2 ppm (one of the aromatic signals is covered due to the solvent); IR (KBr): $\tilde{\nu}$ = 3027, 2925, 2853, 1752, 1655, 1552, 1203 cm^{-1}; ESI-MS: m/z = 1251.42 [M+1]$^+$.

General Procedure for Preparation of Compounds 1 and 2. Aldehyde (**21a**,**b**, 1.0 equiv) was dissolved in toluene, and then a solution of cyanoacetic acid (1.3 equiv) and piperidine (1.0 equiv) in MeCN was added. The resulting mixture was heated to 70 °C and stirred for 5 h, and then chloroform (100 mL) and a 3 M aqueous solution of HCl (100 mL) were added. The organic phase was separated, and the solvent was evaporated. The resulting solid was purified by

DOI: 10.1021/acsomega.8b03560
ACS Omega 2019, 4, 7614−7627

consecutive washes with pentane, diethyl ether, methanol, and ethyl acetate and dried under vacuum.

*2-Cyano-3-(5-(5-((3E)-3-(2-oxo-5-(5-(4-(diphenylamino) phenyl)-3,4-dihexylthiophen-2-yl)-furan-3(2H)-ylidene)-furan-2(3H)-on-5-yl)-3,4-dihexylthiophen-2-yl)thiophen-2-yl)acrylic acid (**1**).* Aldehyde **21a** (30 mg, 0.029 mmol) was dissolved in toluene (4 mL) and reacted with cyanoacetic acid (3.2 mg, 0.038 mmol) and piperidine (2.5 mg, 0.029 mmol, 2.9 μL) in MeCN (2.0 mL). Workup and purification afforded compound **1** (12 mg, 0.011 mmol, 37% yield) as an amorphous dark solid. ^{1}H-NMR (300 MHz, THF-d_8): δ = 8.37 (s, 1H), 7.80−7.91 (m, 1H), 7.43−7.52 (m, 1H), 7.22−7.41 (m, 8H), 6.99−7.19 (m, 8H), 2.81−2.97 (m, 6H), 2.61−2.74 (m, 2H), 1.51−1.68 (m, 12H), 1.21−1.49 (m, 20H), 0.79−0.98 (m, 12H) ppm; ^{13}C−NMR (75 MHz, THF-d_8): δ = 166.8, 166.6, 163.7, 155.5, 153.3, 149.2, 149.0, 148.2, 148.1, 146.1, 145.9, 144.6, 144.2, 141.5, 139.9, 139.1, 137.5, 135.6, 130.4, 130.1, 128.0, 127.8, 126.9, 125.8, 124.6, 124.4, 123.9, 122.8, 116.4, 105.6, 104.3, 100.5, 32.4, 32.3, 32.2, 31.5, 31.2, 30.6, 30.48, 30.46, 30.41, 30.3, 30.1, 29.8, 29.5, 28.9, 27.9, 23.4, 23.34, 23.30, 14.3 ppm; IR (KBr): $\tilde{\nu}$ = 3421, 3067, 2923, 2853, 2211, 1759, 1552, 1201 cm^{-1}; ESI-MS: m/z = 1084.93 [M]$^+$; HRMS (ESI) $C_{66}H_{72}O_6N_2S_3$ ([M]$^+$), calcd 1084.4547, found 1084.4527.

*2-Cyano-3-(5-(5-((3E)-3-(2-oxo-5-(5-(4-(bis(4-(Hexylthio) phenyl)amino)phenyl)-3,4-dihexylthiophen-2-yl)-furan-3(2H)-ylidene)-furan-2(3H)-on-5-yl)-3,4-dihexylthiophen-2-yl) thiophen-2-yl)acrylic acid (**2**).* Aldehyde **21b** (50 mg, 0.040 mmol) was dissolved in toluene (6.0 mL) and reacted with cyanoacetic acid (4.4 mg, 0.052 mmol) and piperidine (3.4 mg, 0.040 mmol, 4.0 μL) in MeCN (3.0 mL). Workup and purification afforded compound **2** (33 mg, 0.025 mmol, 62% yield) as a dark gummy solid. ^{1}H-NMR (300 MHz, THF-d_8): δ = 8.34 (s, 1H), 7.83 (d, J = 3.9 Hz, 1H), 7.45 (d, J = 3.9 Hz, 1H), 7.19−7.41 (m, 8H), 6.98−7.13 (m, 6H), 2.79−2.98 (m, 10H), 2.60−2.74 (m, 2H), 1.54−1.68 (m, 12H), 1.22−1.48 (m, 36H), 0.83−0.98 (m, 18H) ppm; ^{13}C-NMR (75 MHz, THF-d_8): δ = 166.7, 166.5, 163.6, 155.4, 153.3, 149.0, 148.7, 148.3, 145.90, 145.87, 145.7, 144.6, 144.2, 141.5, 139.1, 137.5, 135.6, 132.9, 131.1, 130.5, 128.00, 127.96, 126.9, 126.1, 125.8, 124.7, 123.9, 122.8, 116.4, 105.6, 104.3, 100.4, 34.5, 32.4, 32.3, 32.2, 30.51, 30.47, 30.43, 30.3, 30.1, 30.0, 29.2, 23.43, 23.41, 23.36, 23.32, 23.29, 14.3, 14.2 ppm; IR (KBr): $\tilde{\nu}$ = 3435, 2924, 2853, 2212, 1760, 1522, 1201 cm^{-1}; ESI-MS: m/z = 1316.41 [M]$^+$. HRMS (ESI) $C_{78}H_{96}O_6N_2S_5$ ([M]$^+$), calcd 1316.5866, found 1316.5862.

Preparation of Compound 6. *4-(5-((3E)-3-(2-Oxo-5-(5-(4-(bis(4-(hexylthio)phenyl)amino) phenyl)-3,4-dihexylthiophen-2-yl)-furan-3(2H)-ylidene)-furan-2(3H)-on-5-yl)-3,4-dihexyl thiophen-2-yl)benzoic acid (**6**).* Bromide **19b** (55 mg, 0.045 mmol, 1.0 equiv) and 4-(tributyltin)benzoic acid (**22**, 37 mg, 0.090 mmol, 2.0 equiv) were dissolved in toluene (2.0 mL) and stirred with a solution of Pd_2dba_3 (2.3 mg, 0.0023 mmol, 5 mol %) and P(2-furyl)$_3$ (1.0 mg, 0.0045 mmol, 10 mol %) in toluene (2 mL) at 80 °C for 7 h. After cooling to room temperature, the solvent was evaporated under reduced pressure. The crude product was first purified by flash column chromatography (dichloromethane, then ethyl acetate, and then ethyl acetate + 2% acetic acid). The solid obtained was dissolved in dichloromethane (20 mL), washed with 3 M aq HCl (25 mL), and dried with Na_2SO_4. After filtration and removal of the solvent, the solid residue was washed with small portions of pentane (3 × 5 mL) and methanol (2 × 5 mL) to give dye **6** (45 mg, 0.036 mmol, 79% yield) as a blue gummy solid. ^{1}H-NMR (400 MHz, $CDCl_3$): δ = 8.18 (d, J = 7.9 Hz, 2H), 7.57 (d, J = 7.9 Hz, 2H), 7.24−7.32 (m, 8H), 7.03−7.10 (m, 6H), 2.76−2.95 (m, 8H), 2.56−2.72 (m, 4H), 1.19−1.82 (m, 48H), 0.85−1.00 (m, 18H); ^{13}C-NMR (100 MHz, $CDCl_3$): δ = 170.8, 167.2, 167.1, 154.7, 153.6, 148.5, 147.8, 147.6, 145.2, 145.1, 142.3, 142.1, 141.0, 139.8, 131.5, 130.8, 130.0, 129.3, 127.6, 126.0, 125.4, 125.0, 124.1, 123.7, 122.6, 104.5, 104.0, 34.5, 31.6, 31.5, 31.0, 30.2, 29.8, 29.5, 29.3, 28.6, 27.4, 22.8, 22.7, 14.2, 14.1 (two of the aromatic signals are absent due to overlapping); IR (KBr): $\tilde{\nu}$ = 3418, 2958, 2924, 2855, 1762, 1694, 1557, 1464, 1200 cm^{-1}; ESI-MS: m/z = 1260.72 [M+1]$^+$. HRMS (ESI) $C_{77}H_{97}NO_6S_4$ ([M]$^+$), calcd 1259.6199, found 1259.6189.

Preparation of Compound 7. *4-((5-((3E)-3-(2-Oxo-5-(5-(4-(bis(4-(hexylthio)phenyl) amino)phenyl)-3,4-dihexylthiophen-2-yl)-furan-3(2H)-ylidene)-furan-2(3H)-on-5-yl)-3,4-dihexylthiophen-2-yl)ethynyl) benzoic acid (**7**).* A solution of bromide **21b** (75 mg, 0.061 mmol, 1.0 equiv) in THF (9.0 mL) was degassed, and then 4-ethynylbenzoic acid (**23**, 36 mg, 0.246 mmol, 4.0 equiv), $Pd(PPh_3)_4$ (6.1 mg, 0.0061 mmol, 10 mol %), copper (I) iodide (1.2 mg, 0.0061 mmol, 10 mol %), and triethylamine (0.35 mL) were added. The resulting mixture was stirred at 50 °C for 1 h, and then after cooling to room temperature, the solvent was removed under reduced pressure. The reaction crude was suspended in dichloromethane (25 mL) and 3 M aq HCl (25 mL) and filtered over Celite. The organic phase was washed again with 3 M aq HCl (25 mL) and dried. The crude obtained after solvent removal was filtered by flash column chromatography (dichloromethane, then ethyl acetate, and then ethyl acetate + 2% acetic acid). The solid obtained was dissolved in dichloromethane (25 mL), and the organic phase was washed with 3 M aq HCl (25 mL) and dried. After filtration and removal of the solvent, the residue was washed with pentane (3 × 5 mL) and methanol (2 × 5 mL) to give dye **7** (55 mg, 0.043 mmol, 70% yield) as a blue gummy solid. ^{1}H-NMR (400 MHz, $CDCl_3$): δ = 8.06 (d, J = 8.0 Hz, 2H), 7.56 (d, J = 8.0 Hz, 2H), 7.22−7.30 (m, 8H), 7.02−7.08 (m, 6H), 2.89 (t, J = 7.3 Hz, 4H), 2.78−2.86 (m, 4H), 2.69−2.78 (m, 2H), 2.57−2.63 (m, 2H), 1.21−1.72 (m, 48H), 0.82−1.01 (m, 18H); ^{13}C-NMR (100 MHz, $CDCl_3$): δ = 170.8, 167.0, 166.9, 154.8, 152.7, 150.4, 148.8, 147.8,145.6, 145.4, 145.2, 141.0, 131.6, 131.3, 130.8, 130.3, 129.9, 128.8, 128.3, 127.5, 127.3, 125.4, 125.2, 124.1, 123.3, 122.9, 122.5, 105.1, 104.2, 98.9, 86.4, 34.5, 31.7, 31.6, 31.5, 31.0, 30.4, 30.1, 29.9, 29.8, 29.5, 29.4, 28.7, 22.8, 22.7, 14.2; IR (KBr): $\tilde{\nu}$ = 3418, 2954, 2921, 2853, 2189, 1756, 1694, 1555, 1416, 1201 cm^{-1}. ESI-MS: m/z = 1283.80 [M]$^+$. HRMS (ESI) $C_{79}H_{97}NO_6S_4$ ([M]$^+$), calcd 1283.6199, found 1283.6194.

Preparation of Aza-Pechmann Derivative 8. *(3E)-5,5′-(5-Bromo-3,4-dihexylthiophen-2-yl)-1,1′-dihexyl-3,3′-bipyrrolylidene-2,2′-dione (**24**).* A solution of dibromide **17** (0.200 g, 0.243 mmol, 1.0 equiv), hexylamine (0.098 g, 0.972 mmol, 128 μL, 4.0 equiv), and DMAP (6.0 mg, 0.049 mmol, 20 mol %) in dichloromethane (15 mL) was stirred at room temperature for 16 h, and then p-toluenesulfonic acid monohydrate (0.277 g, 1.458 mmol, 6.0 equiv) was added and let to react for 3 h at room temperature. The organic phase was washed with 0.3 M aq HCl (25 mL), $NaHCO_3$-saturated aqueous solution (25 mL), and brine (25 mL) and then dried. After evaporation of the solvent and flash column chromatography (petroleum ether/toluene = 3/1, then 2/1), compound **24** (76 mg, 0.077 mmol, 31% yield) was obtained as a viscous

DOI: 10.1021/acsomega.8b03560
ACS Omega 2019, 4, 7614−7627

purple oil. ^{1}H-NMR (400 MHz, $CDCl_3$): δ = 6.87 (s, 2H), 3.55 (t, J = 7.3 Hz, 4H), 2.62 (t, J = 7.6 Hz, 4H), 2.56 (t, J = 7.6 Hz, 4H), 1.17−1.53 (m, 48H), 0.82−0.93 (m, 18H); ^{13}C-NMR (100 MHz, $CDCl_3$): δ = 170.4, 145.3, 143.8, 142.7, 128.6, 126.5, 112.6, 105.4, 41.1, 31.7, 31.6, 31.4, 30.9, 29.6, 29.4, 29.2, 29.0, 28.7, 26.5, 22.7, 22.6, 14.2; IR (KBr): $\tilde{\nu}$ = 3036, 2955, 2925, 2855, 1674, 1493, 1278 cm^{-1}; ESI-MS: m/z = 989.56 $[M+1]^+$.

*(3E)-5-(5-(4-(Diphenylamino)phenyl)-3,4-dihexylthiophen-2-yl)-5′-(5-bromo-3,4-dihexylthiophen-2-yl)-1,1′-dihexyl-3,3′-bipyrrolylidene-2,2′-dione (**26**).* Dibromide **24** (203 mg, 0.21 mmol, 1.0 equiv) was dissolved in toluene (5.0 mL) and reacted with a solution of Pd_2dba_3 (0.011 g, 0.010 mmol, 5 mol %), P(2-furyl)$_3$ (4.8 mg, 0.021 mmol, 10 mol %), and 4-tributylstannyl-*N*,*N*-diphenylaniline (**18a**, 109 mg, 0.21mmol, 1.0 equiv) in toluene (5.0 mL). The mixture was heated to 85 °C, stirred for 7 h, and then after cooling to rt, diluted with H_2O (30 mL) and ethyl acetate (50 mL). The organic layers were washed with brine (30 mL) and dried. After filtration, evaporation of the solvent gave a dark-purple crude which was purified by flash column chromatography (petroleum ether/toluene 4:1 to 3:2) to give pure product **26** (67 mg, 0.058 mmol, 28% yield) as a dark-purple gummy solid. ^{1}H-NMR (400 MHz, $CDCl_3$): δ = 7.26−7.31 (m, 6H), 7.14 (d, J = 7.6 Hz, 4H), 7.04−7.11 (m, 4H), 6.94 (s, 1H), 6.88 (s, 1H), 3.65 (t, J = 7.4 Hz, 2H), 3.56 (t, J = 7.4 Hz, 2H), 2.68 (t, J = 7.7 Hz, 2H), 2.62 (t, J = 7.7 Hz, 4H), 2.56 (t, J = 7.8 Hz, 2H), 1.17−1.51 (m, 48H), 0.78−0.93 (m, 18H); ^{13}C-NMR (100 MHz, $CDCl_3$): δ = 170.8, 170.4, 147.7, 147.6, 146.9, 145.3, 144.4, 143.6, 142.6, 141.1, 139.0, 130.1, 129.5,129.1, 128.0, 127.8, 126.7, 124.9, 124.6, 123.5, 123.0, 112.3, 105.5, 104.9, 41.2, 41.0, 31.7, 31.6, 31.5, 31.4, 31.1, 30.9, 29.9, 29.63, 29.58, 29.5, 29.4, 29.3, 29.2, 29.0, 28.8, 28.7, 27.6, 26.5, 22.8, 22.7, 22.6, 14.2, 14.1; IR (KBr): $\tilde{\nu}$ = 3033, 2956, 2926, 2855, 1673, 1494, 1279 cm^{-1}; ESI-MS: m/z = 1153.76 $[M]^+$.

*(3E)-5-(5-(4-(Diphenylamino)phenyl)-3,4-dihexylthiophen-2-yl)-5′-(5-(5-formylthiophen-2-yl)-3,4-dihexylthiophen-2-yl)-1,1′-dihexyl-3,3′-bipyrrolylidene-2,2′-dione (**27**).* Bromide **26** (67 mg, 0.058 mmol, 1.0 equiv) was dissolved in toluene (2.0 mL) and then reacted with a solution of Pd_2dba_3 (4.7 mg, 4.3 μmol, 7.5 mol %), P(2-furyl)$_3$ (2.0 mg, 8.7 μmol, 15 mol %), and 2-tributylstannyl-5-formylthiophene (**20**, 47 mg, 0.12 mmol, 2.0 equiv) in toluene (3.0 mL). The reaction mixture was heated to 110 °C under stirring for 24 h, then cooled, and diluted with water (30 mL) and dichloromethane (30 mL). The organic phase was washed with brine (30 mL) and dried. After removal of the solvent under vacuum, purification by flash column chromatography (petroleum ether/toluene 1:1, then toluene) gave pure aldehyde **27** (35 mg, 0.030 mmol, 51% yield) as a dark-blue gummy solid. ^{1}H-NMR (400 MHz, $CDCl_3$): δ = 9.91 (s, 1H), 7.73 (d, J = 3.9 Hz, 1H), 7.26−7.31 (m, 6H), 7.14 (d, J = 7.7 Hz, 4H), 7.04−7.11 (m, 5H), 6.97 (s, 1H), 6.96 (s, 1H), 3.61−3.69 (m, 4H), 2.79 (t, J = 7.9 Hz, 2H), 2.60−2.71 (m, 6H), 1.15−1.53 (m, 48H), 0.80−0.92 (m, 18H); ^{13}C-NMR (100 MHz, $CDCl_3$): δ = 182.8, 170.8, 170.5, 147.7, 147.6, 147.1, 145.8, 145.6, 145.4, 144.3, 143.0, 142.3, 141.2, 139.1, 136.9, 132.0, 130.1, 129.5, 129.2, 127.9, 127.7, 127.5, 126.9, 124.9, 124.6, 123.5, 122.9, 105.7, 105.0, 41.2, 31.6, 31.5, 31.4, 31.1, 31.0, 30.9, 30.6, 29.8, 29.7, 29.6, 29.5, 29.3, 29.2, 28.8, 28.6, 28.4, 27.6, 26.5, 22.7, 22.6, 14.2, 14.1; IR (KBr): $\tilde{\nu}$ = 2956, 2927, 2857, 1668, 1629, 1494, 1464, 1279 cm^{-1}; ESI-MS: m/z = 1184.82 $[M+1]^+$; 1201.37 $[M+H_2O]^+$.

*2-Cyano-3-(5-(5-((3E)-1-hexyl-3-(1-hexyl-2-oxo-5-(5-(4-(diphenylamino)phenyl)-3,4-dihexylthiophen-2-yl)-pyrrol-3(2H)-ylidene)-pyrrol-2(3H)-on-5-yl)-3,4-dihexylthiophen-2-yl)thiophen-2-yl)acrylic acid (**8**).* Aldehyde **27** (20 mg, 0.017 mmol, 1.0 equiv) was dissolved in toluene (2.0 mL), and then a solution of cyanoacetic acid (4.3 mg, 0.051 mmol, 3.0 equiv) and piperidine (4.3 mg, 0.051 mmol, 5.0 μL, 3.0 equiv) in MeCN (1.0 mL) was added. The resulting mixture was heated to 75 °C and stirred for 4 h. The solvent was evaporated under vacuum, and the residue was dissolved in dichloromethane (50 mL) and washed with a 3 M aqueous solution of HCl (2 × 50 mL). Evaporation of the solvent gave a green solid, which was purified by consecutive washes with pentane, diethyl ether, and methanol and dried under vacuum to afford acid **8** (17 mg, 0.014 mmol, 81% yield) as a dark-green gummy solid. ^{1}H-NMR (400 MHz, THF-d_8): δ = 8.39 (s, 1H), 7.84−7.90 (m, 1H), 7.40−7.44 (m, 1H), 7.35 (d, J = 8.2 Hz, 2H), 7.21−7.31 (m, 5H), 6.94−7.14 (m, 9H), 3.64−3.75 (m, 4H), 2.84−2.98 (m, 2H), 2.65−2.82 (m, 6H), 1.20−1.62 (m, 48H), 0.81−0.95 (m, 18H)^{13};C−NMR (100 MHz, THF-d_8): δ = 170.6, 170.4, 163.7, 148.7, 148.3, 147.2, 146.3, 146.1, 145.8, 145.1, 144.9, 142.9, 141.9, 139.6, 139.0, 137.0, 133.0, 130.6, 130.0, 129.1, 128.4, 128.3, 127.6, 125.5, 125.2, 124.1, 123.7, 123.3, 116.4, 106.0, 105.2, 100.2, 41.3, 32.3, 32.2, 32.0, 31.7, 31.6, 31.5, 31.3, 30.5, 30.2, 30.1, 29.8, 29.4, 29.2, 29.0, 28.0, 27.0, 23.3, 23.2, 14.2, 14.1; IR (KBr): $\tilde{\nu}$ = 3459, 2953, 2923, 2851, 2209, 1671, 1632, 1493, 1372, 1259 cm^{-1}; ESI-MS: m/z = 1250.66 $[M]^+$. HRMS (ESI) $C_{78}H_{98}O_4N_4S_3$ ($[M]^+$), calcd 1250.6750, found 1250.6756.

■ ASSOCIATED CONTENT

Supporting Information

The Supporting Information is available free of charge on the ACS Publications website at DOI: 10.1021/acsomega.8b03560.

^{1}H- and ^{13}C-NMR spectra of compounds **19a**, **19b**, **21a**, **21b**, **1**, **2**, **6**, **7**, **24**, **26**, **27**, **8**; UV−vis absorption spectra, fluorescence emission spectra ,and cyclic voltammograms of compounds **1**, **2**, **6**, **7**, and **8**; TD-DFT (CAM-B3LYP/6-31G*)-computed absorption maxima (λ^a_{max}), excitation energy (E_{exc}), and oscillator strengths (f) of reaction intermediates **16**, **17**, **19a**, and **21a** and dye **1**; and fabrication details and characterization of dye-sensitized solar cells (PDF)

■ AUTHOR INFORMATION

Corresponding Authors

*E-mail: a.dessi@iccom.cnr.it (A.D.).

*E-mail: gianna.reginato@iccom.cnr.it (G.R.).

ORCID

Alessio Dessì: 0000-0003-2358-227X

Gianna Reginato: 0000-0002-7712-3426

Notes

The authors declare no competing financial interest.

■ ACKNOWLEDGMENTS

The authors are grateful to Regione Toscana (FAR-FAS 2014 "SELFIE" Project) and Ente Cassa di Risparmio di Firenze ("ENERGYLAB" Project) for financial support. A.S., S.M., and R.B. thank CINECA and C.R.E.A. for the availability of high-performance computing and MIUR Grant - Department of

DOI: 10.1021/acsomega.8b03560
ACS Omega 2019, 4, 7614−7627

Excellence 2018-2022. S.M. is grateful for the Ph.D. grant within the Progetto Pegaso funded by Regione Toscana. We thank Mr. Carlo Bartoli (CNR-ICCOM) for technical support.

■ ADDITIONAL NOTE

[1]The moderate yield of compound **1** could be ascribed to its low solubility, which hampered its final purification.

■ REFERENCES

(1) Hagfeldt, A.; Boschloo, G.; Sun, L.; Kloo, L.; Pettersson, H. Dye-Sensitized Solar Cells. *Chem. Rev.* **2010**, *110*, 6595.
(2) O'Regan, B.; Grätzel, M. A low-cost, high-efficiency solar cell based on dye-sensitized colloidal TiO_2 films. *Nature* **1991**, *353*, 737.
(3) Mishra, A.; Fischer, M. K. R.; Bäuerle, P. Metal-Free Organic Dyes for Dye-Sensitized Solar Cells: From Structure: Property Relationships to Design Rules. *Angew. Chem., Int. Ed.* **2009**, *48*, 2474.
(4) Bessho, T.; Zakeeruddin, S. M.; Yeh, C.-Y.; Diau, E. W.-G.; Grätzel, M. Highly Efficient Mesoscopic Dye-Sensitized Solar Cells Based on Donor−Acceptor-Substituted Porphyrins. *Angew. Chem., Int. Ed.* **2010**, *49*, 6646.
(5) Yao, Z.; Zhang, M.; Wu, H.; Yang, L.; Li, R.; Wang, P. Donor/Acceptor Indenoperylene Dye for Highly Efficient Organic Dye-Sensitized Solar Cells. *J. Am. Chem. Soc.* **2015**, *137*, 3799.
(6) Kakiage, K.; Aoyama, Y.; Yano, T.; Oya, K.; Fujisawa, J.-i.; Hanaya, M. Highly-efficient dye-sensitized solar cells with collaborative sensitization by silyl-anchor and carboxy-anchor dyes. *Chem. Commun.* **2015**, *51*, 15894.
(7) Brogdon, P.; Cheema, H.; Delcamp, J. H. Near-Infrared-Absorbing Metal-Free Organic, Porphyrin, and Phthalocyanine Sensitizers for Panchromatic Dye-Sensitized Solar Cells. *ChemSusChem* **2018**, *11*, 86.
(8) (a) Burke, A.; Schmidt-Mende, L.; Ito, S.; Grätzel, M. A novel blue dye for near-IR 'dye-sensitised' solar cell applications. *Chem. Commun.* **2007**, 234. (b) Paek, S.; Choi, H.; Kim, C.; Cho, N.; So, S.; Song, K.; Nazeeruddin, M. K.; Ko, J. Efficient and stable panchromatic squaraine dyes for dye-sensitized solar cells. *Chem. Commun.* **2011**, *47*, 2874. (c) Shi, Y.; Hill, R. B. M.; Yum, J.-H.; Dualeh, A.; Barlow, S.; Gratzel, M.; Marder, S. R.; Nazeeruddin, M. K. A high-efficiency panchromatic squaraine sensitizer for dye-sensitized solar cells. *Angew. Chem., Int. Ed.* **2011**, *50*, 6619. (d) Jradi, F. M.; Kang, X.; O'Neil, D.; Pajares, G.; Getmanenko, Y. A.; Szymanski, P.; Parker, T. C.; El-Sayed, M. A.; Marder, S. R. Near-Infrared Asymmetrical Squaraine Sensitizers for Highly Efficient Dye Sensitized Solar Cells: The Effect of π-Bridges and Anchoring Groups on Solar Cell Performance. *Chem. Mater.* **2015**, *27*, 2480.
(9) Hao, Y.; Saygili, Y.; Cong, J.; Eriksson, A.; Yang, W.; Zhang, J.; Polanski, E.; Nonomura, K.; Zakeeruddin, S. M.; Gratzel, M.; Hagfeldt, A.; Boschloo, G. Novel Blue Organic Dye for Dye-Sensitized Solar Cells Achieving High Efficiency in Cobalt-Based Electrolytes and by Co-Sensitization. *ACS Appl. Mater. Interfaces* **2016**, *8*, 32797.
(10) Yum, J.-H.; Holcombe, T. W.; Kim, Y.; Rakstys, K.; Moehl, T.; Teuscher, J.; Delcamp, J. H.; Nazeeruddin, M. K.; Grätzel, M. Blue-Coloured Highly Efficient Dye-Sensitized Solar Cells by Implementing the Diketopyrrolopyrrole Chromophore. *Sci. Rep.* **2013**, *3*, 2446.
(11) Ren, Y.; Sun, D.; Cao, Y.; Tsao, H. N.; Yuan, Y.; Zakeeruddin, S. M.; Wang, P.; Grätzel, M. A Stable Blue Photosensitizer for Color Palette of Dye-Sensitized Solar Cells Reaching 12.6% Efficiency. *J. Am. Chem. Soc.* **2018**, *140*, 2405.
(12) (a) Norsten, T. B.; Kantchev, E. A. B.; Sullivan, M. B. Thiophene-Containing Pechmann Dye Derivatives. *Org. Lett.* **2010**, *12*, 4816. (b) Kantchev, E. A. B.; Norsten, T. B.; Tan, M. L. Y.; Ng, J. J. Y.; Sullivan, M. B. Thiophene-Containing Pechmann Dyes and Related Compounds: Synthesis, and Experimental and DFT Characterisation. *Chem. - Eur. J.* **2012**, *18*, 695.
(13) (a) Kantchev, E. A. B.; Norsten, T. B.; Sullivan, M. B. Time-dependent density functional theory (TDDFT) modelling of Pechmann dyes: from accurate absorption maximum prediction to virtual dye screening. *Org. Biomol. Chem.* **2012**, *10*, 6682. (b) Hashimoto, H.; Shiratori, K.; Kawakita, K.; Tanaka, T.; Sekine, R.; Irikawa, H. Preparation and Properties of Dehydrotrichotomine-type Dyes: A New Near-Infrared Absorbing Indigoid. *Heterocycles* **2005**, *65*, 1385.
(14) (a) Efrem, A.; Courté, M.; Wang, K.; Fichou, D.; Wang, M. Synthesis and characterization of γ-lactone-Pechmann dye based donor-acceptor conjugated polymers. *Dyes Pigm.* **2016**, *134*, 171. (b) Cai, Z.; Luo, H.; Qi, P.; Wang, J.; Zhang, G.; Liu, Z.; Zhang, D. Alternating Conjugated Electron Donor−Acceptor Polymers Entailing Pechmann Dye Framework as the Electron Acceptor Moieties for High Performance Organic Semiconductors with Tunable Characteristics. *Macromolecules* **2014**, *47*, 2899. (c) Cai, Z.; Liu, Z.; Luo, H.; Qi, P.; Zhang, G.; Zhang, D. π-Extented Conjugated Polymers Entailing Pechmann Dye Moieties for Solution-Processed Ambipolar Organic Semiconductors. *Chin. J. Chem.* **2014**, *32*, 788.
(15) Hayashi, M.; Toshimitsu, F.; Sakamoto, R.; Nishihara, H. Double Lactonization in Triarylamine-Conjugated Dimethyl Diethynylfumarate: Formation of Intensely Colored and Luminescent Quadrupolar Molecules Including a Missing Structural Isomer of Pechmann Dyes. *J. Am. Chem. Soc.* **2011**, *133*, 14518.
(16) Qi, P.; Wang, Z.; Liu, Z.; Yang, S.; Yang, Y.; Yao, J.; Zhang, G.; Zhang, D. Conjugated donor−acceptor terpolymers entailing the Pechmann dye and dithienyl-diketopyrrolopyrrole as co-electron acceptors: tuning HOMO/LUMO energies and photovoltaic performances. *Polym. Chem.* **2016**, *7*, 3838.
(17) (a) Cai, Z.; Guo, Y.; Yang, S.; Peng, Q.; Luo, H.; Liu, Z.; Zhang, G.; Liu, Y.; Zhang, D. New Donor−Acceptor−Donor Molecules with Pechmann Dye as the Core Moiety for Solution-Processed Good-Performance Organic Field-Effect Transistors. *Chem. Mater.* **2013**, *25*, 471. (b) Luo, H.; Dong, X.; Cai, Z.; Wang, L.; Liu, Z. Pechmann Dye-Based Molecules Containing Fluorobenzene Moieties for Ambipolar Organic Semiconductors. *Asian J. Org. Chem.* **2018**, *7*, 592.
(18) (a) Zhu, W.; Wu, Y.; Wang, S.; Li, W.; Li, X.; Chen, J.; Wang, Z. S.; Tian, H. Organic D-A-π-A Solar Cell Sensitizers with Improved Stability and Spectral Response. *Adv. Funct. Mater.* **2011**, *21*, 756. (b) Wu, Y.; Zhu, W. H.; Zakeeruddin, S. M.; Grätzel, M. Insight into D−A−π−A Structured Sensitizers: A Promising Route to Highly Efficient and Stable Dye-Sensitized Solar Cells. *ACS Appl. Mater. Interfaces* **2015**, *7*, 9307. (c) Gao, Y.; Li, X.; Hu, Y.; Fan, Y.; Yuan, J.; Robertson, N.; Hua, J.; Marder, S. R. Effect of an auxiliary acceptor on D−A−π−A sensitizers for highly efficient and stable dye-sensitized solar cells. *J. Mater. Chem. A* **2016**, *4*, 12865. (d) Liyanage, P. N.; Yella, A.; Nazeeruddin, M.; Grätzel, M.; Delcamp, J. H. Thieno[3,4-*b*]pyrazine as an Electron Deficient π-Bridge in D−A−π−*A* DSCs. *ACS Appl. Mater. Interfaces* **2016**, *8*, 5376.
(19) (a) Dessì, A.; Calamante, M.; Mordini, A.; Peruzzini, M.; Sinicropi, A.; Basosi, R.; de Biani, F. F.; Taddei, M.; Colonna, D.; di Carlo, A.; Reginato, G.; Zani, L. Thiazolo[5,4-*d*]thiazole-based organic sensitizers with strong visible light absorption for transparent, efficient and stable dye-sensitized solar cells. *RSC Adv.* **2015**, *5*, 32657. (b) Dessì, A.; Calamante, M.; Mordini, A.; Peruzzini, M.; Sinicropi, A.; Basosi, R.; de Biani, F. F.; Taddei, M.; Colonna, D.; Di Carlo, A.; Reginato, G.; Zani, L. Organic dyes with intense light absorption especially suitable for application in thin-layer dye-sensitized solar cells. *Chem. Commun.* **2014**, *50*, 13952. (c) Bernini, C.; Zani, L.; Calamante, M.; Reginato, G.; Mordini, A.; Taddei, M.; Basosi, R.; Sinicropi, A. Excited State Geometries and Vertical Emission Energies of Solvated Dyes for DSSC: A PCM/TD-DFT Benchmark Study. *J. Chem. Theory Comput.* **2014**, *10*, 3925.
(20) Otsuka, A.; Funabiki, K.; Sugiyama, N.; Mase, H.; Yoshida, T.; Minoura, H.; Matsui, M. Design and Synthesis of Near-infrared-active Heptamethine−Cyanine Dyes to Suppress Aggregation in a Dye-sensitized Porous Zinc Oxide Solar Cell. *Chem. Lett.* **2008**, *37*, 176.
(21) Robson, K. C. D.; Hu, K.; Meyer, G. J.; Berlinguette, C. P. Atomic Level Resolution of Dye Regeneration in the Dye-Sensitized Solar Cell. *J. Am. Chem. Soc.* **2013**, *135*, 1961.

DOI: 10.1021/acsomega.8b03560
ACS Omega 2019, 4, 7614−7627

(22) Frisch, M. J.; Trucks, G. W.; Schlegel, H. B.; Scuseria, G. E.; Robb, M. A.; Cheeseman, J. R.; Scalmani, V.; Barone, V.; Mennucci, B.; Petersson, G. A.; Nakatsuji, H.; Caricato, M.; Li, X.; Hratchian, H. P.; Izmaylov, A. F.; Bloino, J.; Zheng, G.; Sonnenberg, J. L.; Hada, M.; Ehara, M.; Toyota, K.; Fukuda, R.; Hasegawa, J.; Ishida, M.; Nakajima, T.; Honda, Y.; Kitao, O.; Nakai, H.; Vreven, T.; Montgomery, J. A., Jr.; Peralta, J. E.; Ogliaro, F.; Bearpark, M.; Heyd, J. J.; Brothers, E.; Kudin, K. N.; Staroverov, V. N.; Kobayashi, R.; Normand, J.; Raghavachari, K.; Rendell, A.; Burant, J. C.; Iyengar, S. S.; Tomasi, J.; Cossi, M.; Rega, N.; Millam, N. J.; Klene, M.; Knox, J. E.; Cross, J. B.; Bakken, V.; Adamo, C.; Jaramillo, J.; Gomperts, R.; Stratmann, R. E.; Yazyev, O.; Austin, A. J.; Cammi, R.; Pomelli, C.; Ochterski, J. W.; Martin, R. L.; Morokuma, K.; Zakrzewski, V. G.; Voth, G. A.; Salvador, P.; Dannenberg, J. J.; Dapprich, S.; Daniels, A. D.; Farkas, Ö.; Foresman, J. B.; Ortiz, J. V.; Cioslowski, J.; Fox, D. J., *Gaussian 09*. Gaussian, Inc., Wallingford CT, 2009, (Revision C.01).

(23) (a) Becke, A. D. Density-functional thermochemistry. III. The role of exact exchange. *J. Chem. Phys.* **1993**, *98*, 5648. (b) Lee, C.; Yang, W.; Parr, R. G. Development of the Colle-Salvetti correlation-energy formula into a functional of the electron density. *Phys. Rev. B* **1988**, *37*, 785.

(24) Tomasi, J.; Mennucci, B.; Cammi, R. Quantum Mechanical Continuum Solvation Models. *Chem. Rev.* **2005**, *105*, 2999.

(25) Franchi, D.; Calamante, M.; Reginato, G.; Zani, L.; Peruzzini, M.; Taddei, M.; de Biani, F. F.; Basosi, R.; Sinicropi, A.; Colonna, D.; Di Carlo, A.; Mordini, A. A comparison of carboxypyridine isomers as sensitizers for dyesensitized solar cells: assessment of device efficiency and stability. *Tetrahedron* **2014**, *70*, 6285.

(26) Fitri, A.; Benjelloun, A. T.; Benzakour, M.; Mcharfi, M.; Hamidi, M.; Bouachrine, M. Theoretical investigation of new thiazolothiazole-based D-π-A organic dyes for efficient dye-sensitized solar cell. *Spectrochim. Acta, Part A* **2014**, *124*, 646.

(27) Kakiage, K.; Aoyama, Y.; Yano, T.; Otsuka, T.; Kyomen, T.; Unno, M.; Hanaya, M. An achievement of over 12 percent efficiency in an organic dye-sensitized solar cell. *Chem. Commun.* **2014**, *50*, 6379.

(28) (a) Anderson, N. A.; Ai, X.; Chen, D.; Mohler, D. L.; Lian, T. Bridge-Assisted Ultrafast Interfacial Electron Transfer to Nanocrystalline SnO_2 Thin Films. *J. Phys. Chem. B* **2003**, *107*, 14231. (b) Wang, L.; Ernstorfer, R.; Willig, F.; May, V. Absorption Spectra Related to Heterogeneous Electron Transfer Reactions: The Perylene TiO_2 System. *J. Phys. Chem. B* **2005**, *109*, 9589. (c) Ernstorfer, R.; Felber, S.; Storck, W.; Galoppini, E.; Wei, Q.; Willig, F. Distance dependence of heterogeneous electron transfer probed in ultra-high vacuum with femtosecond transient absorption. *Res. Chem. Intermed.* **2005**, *31*, 643.

(29) Dessì, A.; Bartolini, M.; Calamante, M.; Zani, L.; Mordini, A.; Reginato, G. Extending the conjugation of Pechmann lactone thienyl derivatives: a new class of small molecules for organic electronics application. *Synthesis* **2018**, *50*, 1284.

(30) Dessì, A.; Consiglio, G. B.; Calamante, M.; Reginato, G.; Mordini, A.; Peruzzini, M.; Taddei, M.; Sinicropi, A.; Parisi, M. L.; de Biani, F. F.; Basosi, R.; Mori, R.; Spatola, M.; Bruzzi, M.; Zani, L. Organic chromophores based on a fused bis-thiazole core and their application in dye-sensitized solar cells. *Eur. J. Org. Chem.* **2013**, 1916.

(31) (a) Fujinaga, M.; Yamasaki, T.; Maeda, J.; Yui, J.; Xie, L.; Nagai, Y.; Nengaki, N.; Hatori, A.; Kumata, K.; Kawamura, K.; Zhang, M.-R. Development of *N*-[4-[6-(Isopropylamino)pyrimidin-4-yl]-1,3-thiazol-2-yl]-*N*-methyl-4-[^{11}C]methylbenzamide for Positron Emission Tomography Imaging of Metabotropic Glutamate 1 Receptor in Monkey Brain. *J. Med. Chem.* **2012**, *55*, 11042. (b) Tang, P.; Furuya, T.; Ritter, T. Silver-Catalyzed Late-Stage Fluorination. *J. Am. Chem. Soc.* **2010**, *132*, 12150.

(32) (a) Chinchilla, R.; Nájera, C. The Sonogashira Reaction: A Booming Methodology in Synthetic Organic Chemistry. *Chem. Rev.* **2007**, *107*, 874. (b) Chinchilla, R.; Nájera, C. Recent advances in Sonogashira reactions. *Chem. Soc. Rev.* **2011**, *40*, 5084.

(33) (a) Chen, R.; Yang, X.; Tian, H.; Sun, L. Tetrahydroquinoline dyes with different spacers for organic dye-sensitized solar cells. *J. Photochem. Photobiol., A* **2007**, *189*, 295. (b) Tian, H.; Yang, X.; Chen, R.; Pan, Y.; Li, L.; Hagfeldt, A.; Sun, L. Phenothiazine derivatives for efficient organic dye-sensitized solar cells. *Chem. Commun.* **2007**, 3741. (c) Zhang, L.; Cole, J. M. Dye aggregation in dye-sensitized solar cells. *J. Mater. Chem. A* **2017**, *5*, 19541−19559.

(34) Hardin, B. E.; Snaith, H. J.; McGehee, M. D. The renaissance of dye-sensitized solar cells. *Nat. Photonics* **2012**, *6*, 162.

(35) Boschloo, G.; Hagfeldt, A. Characteristics of the Iodide/Triiodide Redox Mediator in Dye-Sensitized Solar Cells. *Acc. Chem. Res.* **2009**, *42*, 1819−1826.

(36) Koops, S. E.; O'Regan, B. C.; Barnes, P. R. F.; Durrant, J. R. Parameters Influencing the Efficiency of Electron Injection in Dye-Sensitized Solar Cells. *J. Am. Chem. Soc.* **2009**, *131*, 4808.

(37) (a) Peddapuram, A.; Cheema, H.; Adams, R. E.; Schmehl, R. H.; Delcamp, J. H. A Stable Panchromatic Green Dual Acceptor, Dual Donor Organic Dye for Dye-Sensitized Solar Cells. *J. Phys. Chem. C* **2017**, *121*, 8770. (b) Wu, J.; Li, G.; Zhang, L.; Zhou, G.; Wang, Z.-S. Energy level engineering of thieno[3,4-*b*]pyrazine based organic sensitizers for quasi-solid-state dye-sensitized solar cells. *J. Mater. Chem. A* **2016**, *4*, 3342.

(38) Hagberg, D. P.; Yum, J.-H.; Lee, H.; De Angelis, F.; Marinado, T.; Karlsson, K. M.; Humphry-Baker, R.; Sun, L.; Hagfeldt, A.; Grätzel, M.; Nazeeruddin, M. K. Molecular Engineering of Organic Sensitizers for Dye-Sensitized Solar Cell Applications. *J. Am. Chem. Soc.* **2008**, *130*, 6259.

(39) Kopidakis, N.; Neale, N. R.; Frank, A. J. Effect of an Adsorbent on Recombination and Band-Edge Movement in Dye-Sensitized TiO_2 Solar Cells: Evidence for Surface Passivation. *J. Phys. Chem. B* **2006**, *110*, 12485.

(40) Lee, K.-M.; Suryanarayanan, V.; Ho, K.-C.; Thomas, K. R. J.; Lin, J. T. Effects of co-adsorbate and additive on the performance of dye-sensitized solar cells: A photophysical study. *Sol. Energy Mater. Sol. Cells* **2007**, *91*, 1426.

(41) (a) Boschloo, G.; Häggman, L.; Hagfeldt, A. Quantification of the Effect of 4-*tert*-Butylpyridine Addition to I^-/I_3^- Redox Electrolytes in Dye-Sensitized Nanostructured TiO_2 Solar Cells. *J Phys. Chem. B* **2006**, *110*, 13144. (b) Becerril, V. S.; Franchi, D.; Abrahamsson, M. Ionic Liquid-Induced Local Charge Compensation: Effects on Back Electron-Transfer Rates in Dye-Sensitized TiO_2 Thin Films. *J. Phys. Chem. C* **2016**, *120*, 20016.

DOI: 10.1021/acsomega.8b03560
ACS Omega 2019, 4, 7614−7627